Mon. Not. R. astr. Soc. (1989) **240,** 257–284

The colour evolution of high-redshift radio galaxies

J. S. Dunlop,[1] B. Guiderdoni,[2] B. Rocca-Volmerange,[2]
J. A. Peacock[3] and M. S. Longair[3]

[1] *Department of Astronomy, University of Edinburgh, Blackford Hill, Edinburgh EH9 3HJ and School of Physics &Astronomy, Lancashire Polytechnic, Preston PR1 2TQ*
[2] *Institut d'Astrophysique de Paris, CNRS 98 bis Bd. Arago, 75014 Paris, France*
[3] *Royal Observatory, Blackford Hill, Edinburgh EH9 3HJ*

Accepted 1989 March 1. Received 1989 March 1; in original form 1988 November 14

Summary. This paper considers the interpretation of the optical-to-infrared continuum radiation from radio galaxies at large redshift. Using a new sample of ~70 radio galaxies with B, R, and K photometry, we carry out a comparison of observed colours with the predictions of new evolutionary synthesis models. While the bulk of objects at $z \gtrsim 1$ are very red in $R-K$, with most galaxies apparently consistent with 'passive' evolution corresponding to formation redshifts $\gtrsim 5$, *all* high-redshift objects are 'active' in $B-R$. The simplest model to account for these observations is one in which the old and young stellar populations are decoupled: the majority of stars formed at $z \gg 2$, but even the most passive galaxies experience continuing 'low'-level star formation thereafter ($\sim 10^8 \rightarrow 10^9$ $M_\odot$ Gyr^{-1}). Within this framework the bluest $B-R$ colours can be easily reproduced by the further addition of small ($\sim 10^9 \rightarrow 10^{10}$ $M_\odot$ Gyr^{-1}) short-lived (<1 Gyr) starbursts. However, such low-level star-formation activity cannot account for the bluest $R-K$ colours found at $z \sim 1$; the bluest $R-K$ colours imply bulk star-formation at $z \simeq 2$, while the reddest require most of the stars to have formed at $z > 10$. This may genuinely reflect a range of formation redshifts ($z_f \sim 2 \rightarrow 20$), or alternatively a common z_f and very different star-formation histories at intermediate redshifts (e.g. some galaxies experiencing mergers at $z \sim 2$).

1 Introduction

Radio galaxies remain, at present, the only stellar systems which can be located in reasonable numbers at $z \gtrsim 1$. Thus, although they may not be typical of the 'normal' galaxy population, these objects present an opportunity to investigate directly how galaxies have evolved over large look-back times. Radio galaxies have therefore been the subject of increasingly intensive study at optical and infrared wavelengths (e.g. Lilly & Longair 1984; Spinrad 1986; Windhorst, Dressler & Koo 1987), with particular attention being focused on the powerful

3CR sources. The infrared observations of these galaxies (Lilly & Longair 1984) suggested that their spectral evolution may be understood in terms of known changes of stellar populations with time. The most significant conclusions of Lilly & Longair were as follows:

(i) There is no intrinsic change in the infrared colours out to $z \sim 1.2$. This implies that the light seen in the IR window is starlight and that the giant branch in these galaxies is essentially unchanged: even at $z \sim 1$, these objects are relatively old.

(ii) A scatter in optical–infrared colours is seen at high redshift. All galaxies are significantly bluer than the colours predicted by non-evolving models, and the red envelope is well matched by a model of passive evolution. The additional UV flux found in many of the galaxies was interpreted as arising from young starbursts. The UV excess is often found to be distributed throughout the galaxy and is related to the strength of the [O II] 3727 Å emission line, indicating that both might be a measure of the gaseous content of the galaxy.

(iii) The K–z relation is well defined with approximately constant dispersion out to redshifts well in excess of unity, and indicates luminosity evolution of about a magnitude at $z \sim 1$ if $\Omega_0 = 1$. This luminosity evolution can be accounted for simply by passive evolution of the main sequence turn-off mass.

Despite this reassuringly well-behaved evolution in the infrared, more recent detailed optical observations of 3C galaxies have confirmed the suspicion that these are in fact very unusual objects. Particularly significant are the observations that the optical continuum (McCarthy *et al.* 1987; Chambers, Miley & van Breugel 1987) and certainly in some cases the infrared continuum (Chambers, Miley & Joyce 1988) is closely aligned with the axis of the double radio source.

To investigate the extent to which the evolution of the 3CR galaxies may have been affected by their extreme radio powers, it is important to study the spectral evolution of galaxies of lower radio luminosities. Some progress in this direction has been made by the study of the '1-Jy' sample (Lilly, Longair & Allington-Smith 1985). It was found that all the above conclusions are also valid for the '1-Jy' galaxies, but the sample is rather small and still lacks detailed optical data. The present study provides an extension to still lower radio luminosities, being based on the 178-source $S_{2.7\mathrm{GHz}} > 0.1$ Jy Parkes Selected Regions sample (Downes *et al.* 1986; Dunlop *et al.* 1989). This sample was originally chosen for intensive study in order to settle the issue of the high-redshift cut-off in the Radio Luminosity Function (Dunlop & Peacock, in preparation) and we now possess complete photometry at three wavelengths – B, R and K. These multicolour data allow us to carry out a detailed investigation of the star-formation histories of these galaxies because, at $z \sim 1$, the three wavebands B, R, and K sample respectively the very young, intermediate-age, and very old components of the stellar population.

As implied above, it is assumed throughout this study that essentially all of the optical/near-IR light from these distant radio galaxies is indeed starlight. This is obviously not the only possibility – other options (e.g. Tadhunter, Fosbury & di Serego Alighieri 1989) are discussed in Section 5 – but it is the simplest null hypothesis. In any case, it is clearly interesting to investigate what sort of stellar populations are required to reproduce the observed colour evolution of these objects. The interpretation of these new colour data has therefore been carried out using the evolutionary synthesis models of galaxy spectrophotometric evolution developed by Guiderdoni & Rocca-Volmerange (1987). Section 2 discusses these models, and describes the simulation of observable quantities. Section 3 is concerned with the selection of a suitable galaxy subsample for comparison with the theoretical models. In Section 4 these data are compared with the models, and the results discussed. Finally, in Section 5 we summarize our conclusions and consider how they relate to the results of other recent studies.

2 Theoretical modelling of the colour evolution of galaxies

2.1 MODELLING SPECTROPHOTOMETRIC EVOLUTION

The first complete models of spectrophotometric evolution to be developed were those of Bruzual (1983a, b and references therein). These were based on the technique of evolutionary synthesis first introduced by Tinsley (1967, 1972). In this approach, analytical expressions are assumed for both the star-formation rate and the initial mass function. Together, these two functions determine the number of stars of a given mass which are born during a given time interval. Theoretical evolutionary tracks are then used to deduce the amount of time spent by stars of different masses at different positions in the H–R diagram. Models for a single generation of star formation or a continuous star-formation rate can therefore be built, and the stellar population content of the model galaxy determined at any moment in time. Once the stellar content has been determined, the predicted galaxy spectrum is synthesized from a library of observed stellar spectra of different stellar types. The simulation of observable properties such as galaxy colours at high redshift can then be achieved by integrating the spectrum under the relevant broad-band filters after the appropriate redshifting.

Progress in the development of these evolutionary synthesis models is obviously intimately linked to the quality of available spectroscopic data on galaxies and stars of all stellar types, as well as to progress in theories of stellar evolution. Because of the lack of high-quality data outside the optical region, the work prior to Bruzual (e.g. Huchra 1977; Searle, Sargent & Bagnuolo 1973; Tinsley 1980) was limited to predictions of the time dependence of optical magnitudes and colours. It was the new availability of ultraviolet and infrared data which prompted Bruzual to construct the first evolutionary synthesis models which covered the complete UV→IR spectral range. It is clear that a model which extends into the UV is required in order to make predictions in the optical domain at high redshift.

Since the pioneering work of Bruzual, further improvements in the relevant data and theory have occurred but, until recently, no attempt has been made to develop more sophisticated models (although corrections have been added to Bruzual's models, e.g. Chokshi & Wright 1987). In the last few years however, new models of spectrophotometric evolution have been developed by Guiderdoni & Rocca-Volmerange (1987), and it is the results of these models that have been used here to interpret the multicolour photometry of the Parkes Selected Regions radio galaxies. The results of the models have been published in the form of spectra, apparent magnitudes and colours in Rocca-Volmerange & Guiderdoni (1988) and Guiderdoni & Rocca-Volmerange (1988).

2.2 THE MODELS OF SPECTROPHOTOMETRIC EVOLUTION

The main features of the models are as follows.

2.2.1 Star formation

The rate of formation of stars of mass m at time t from the gaseous component of the galaxy is

$$\frac{d\dot{N}(m,t)}{d\ln m} = \phi(m)\ \tau(t), \tag{1}$$

where $\phi(m)$ is the initial mass function ($\phi \propto$ number of stars per interval of ln m), and $\tau(t)$ is the rate of star-formation in units of $M_\odot$ Gyr^{-1}. The adopted IMF is basically that of Scalo (1986) (for massive stars) and has the form $\phi(m) \propto m^{-x}$ with slopes $x = 0.25$, 1.35, 1.7 for the

respective mass ranges $0.1 < m < 1$, $1 < m < 2$, $2 < m < 80\ M_\odot$. The normalization of the IMF is given by

$$\int_{0.1}^{80} \phi(m)\, dm = 0.5 \tag{2}$$

in order to reproduce the observed mass/luminosity ratios (i.e. half the gas goes into stars in this mass range).

2.2.2 *Stellar evolution*

The theoretical stellar-evolution tracks correspond to a helium fraction of $Y = 0.28 \rightarrow 0.30$ and an assumed uniform solar metallicity of $Z = 0.02$. The tracks include four evolutionary stages – main sequence (MS), giant branch (GB), 'red' horizontal branch (HB) (around $\log_{10} T_{\rm eff} = 3.68$) and asymptotic giant branch (AGB). The sources of these tracks are given in Guiderdoni & Rocca-Volmerange (1987). The input tracks are interpolated in mass along each evolutionary stage, in order to get differences in lifetimes lower than 0.2 Gyr for successive masses. For the very short phases, an average luminosity during time step Δt is computed from the total energy released during the phase. Mass loss of massive stars was taken into account according to case B of Maeder (1981). No mass loss during the GB stage was considered for $m < 9\ M_\odot$.

2.2.3 *Synthesis of the galaxy spectrum*

The synthetic spectrum of the stellar population is computed from the distribution of stars in the H–R diagram ($\log_{10} T_{\rm eff} - M_{\rm v}$) using a library of 30 stellar spectra which spans the range of spectral types O5 → M8 and two luminosity classes, V and III (i.e. dwarfs and giants). These spectra cover the spectral range 220–10 680 Å with an average spectral resolution of 10 Å. At wavelengths $\lambda > 1220$ Å the spectra are observational (from the *IUE* Atlases and the library of Gunn & Stryker 1983). The extreme UV range (i.e. $220 \leqslant \lambda \leqslant 1220$ Å) is constructed from theoretical models (Mihalas 1972; Borsenberger & Gros 1978). The IR extension to 25 500 Å is based on stellar *JHK* photometry (Johnson 1966; Lee 1970; Frogel *et al.* 1978; Engels *e al.* 1981), but note that the accuracy of this extension has little impact on the simulation of optical and near-IR magnitudes for galaxies at $z > 1$ (with which this paper is chiefly concerned).

The main differences between this model and that of Bruzual may be summarized as follows (again see Guiderdoni & Rocca-Volmerange 1987 for a full discussion).

(i) The stellar library has a greater resolution (~ 10 Å) than that used by Bruzual (20 → 50 Å) and extends further into the UV, especially for FGK stars.

(ii) Bruzual's model did not include post-GB stages of stellar evolution, in particular the AGB. Also, Bruzual used a unique GB taken from Tinsley & Gunn (1976), whereas the model used here incorporates a mass-dependent GB from Yale tracks computed by Sweigart & Gross (1978). The GB in Bruzual's model is stronger and thus produces *redder* colours at late epochs when it is well developed. This also results in Bruzual's model galaxies being fainter at early epochs when normalization of the models is carried out at the present time.

(iii) The new model adopts the observationally determined IMF of Scalo (1986) in contrast to the single-slope Salpeter (1955) IMF which was used in the original Bruzual models. It is worth noting, however, that Bruzual's models have also been re-run using the multi-slope IMF of Miller & Scalo (1979) – see, for example Bruzual (1985) – with very little change in the colour evolution for early-type galaxies.

(iv) Finally, one of the most important differences concerns the approach taken to the origin of the UV light in elliptical galaxies. It is now well established that the UV flux observed in elliptical galaxies is in excess of the contribution expected from the old Population I which dominates the spectrum in the visible region. The origin of this UV-excess has been a subject of considerable dispute. Bruzual (1985) lists several possible explanations for its origin – the main contenders appear to be young massive main-sequence stars (e.g. Rocca-Volmerange & Guiderdoni 1987), hot HB stars (e.g. Wu *et al.* 1980) or post AGB stars (e.g. Renzini & Buzzoni 1986). Other possible sources of UV flux include blue stragglers, white dwarfs or interacting binaries, but in general it is estimated that the contribution of these objects is below the detected flux level (Wu *et al.* 1980; Renzini 1981). In Bruzual's models the UV light of ellipticals was obtained by 'adding in' a population of hot HB stars. In contrast, the new models account for the UV excess by young stars. The main piece of evidence usually cited in favour of HB stars is that the UV excess appears to be spread evenly throughout the elliptical galaxy. Such a light distribution might be expected to arise more naturally from an evolved population than from young stars. However, recent spectral synthesis studies argue strongly in favour of young main-sequence stars. Rocca-Volmerange & Guiderdoni (1987) have carried out a detailed analysis of the UV spectra of E/S0 galaxies and conclude that the absence of flux between 1900 and 2500 Å indicates that the contribution of HB stars to the UV light is very low. For all the galaxies they analysed, the spectrum in the range $2500 < \lambda < 3100$ Å has a mean spectral type of F8 to G2, indicating relatively recent star formation (~ 5–10 Gyr ago). An additional far-UV excess (i.e. over and above that contributed by the most recent turn-off population) was found only in a subset of their galaxy sample. This fact suggests that the origin of any far-UV excess is more likely to be young main-sequence stars, rather than some evolved population which one would expect to find in *all* elliptical galaxies. Kjaegaard (1987) also concludes, from his spectral analysis of Virgo elliptical galaxies, that the most likely explanation for the UV light seems to be bursts of young stars. Finally, the bulk of galaxies at $z \sim 1$ show more rest-frame UV flux than at the present day. The origin of this light must be young stars, since the contribution of an evolved population such as HB stars should *decrease* with look-back time. It therefore seems more natural to attribute the UV flux seen at the present day also to recently formed main-sequence stars.

2.3 MODELS OF INTEREST IN THE STUDY OF RADIO GALAXIES

Based on the interpretation that the level of galaxy UV light is determined by the current rate of star formation, Guiderdoni & Rocca-Volmerange (1987) have proposed a scheme in which the range of colours of galaxies in the Hubble sequence is reproduced by models with a corresponding range of star-formation laws. Since the host galaxies of radio sources are known to be ellipticals, the models of interest for the present study are the 'UV-Hot' elliptical, the 'UV-Cold' elliptical, and the 1-Gyr 'Burst' model (listed in Table 1). The terms UV-Hot and UV-Cold refer to the two extremes of the range of UV spectra which are observed in ellipticals at

Table 1. The star-formation laws, $\tau(t)$ (per unit mass of galaxy), used in the three alternative models of elliptical galaxy evolution, and the corresponding time-scales t_* for gas consumption. Units of t are Gyr.

Colour class	SFR, $\tau(t)$	t_* (Gyr)	μ
Burst	1 for $t < 1$ Gyr	0.6	1.0
UV-Cold elliptical	$\exp(-t)$	1.0	0.6
UV-Hot elliptical	$0.37 \exp(-0.37t)$	2.7	0.3

the present day (see Rocca-Volmerange & Guiderdoni 1987). The models of the same names have therefore been designed to produce, via the appropriate rate of exponentially decreasing star formation throughout their evolution, the observed extremes of UV-Hot and UV-Cold spectra at the present epoch (i.e. after $t \sim 13$ Gyr of evolution). In terms of the μ parameter introduced by Bruzual, the Hot and Cold elliptical models correspond to $\mu = 0.3$ and 0.6, respectively. The μ-parameter represents the fraction of the initially purely gaseous galaxy which is converted into stars during the first Gyr of its existence, i.e.

$$\mu = \frac{1}{M_{\rm tot}} \int_0^{1\,Gyr} \tau(t)\, dt, \tag{5}$$

where $\tau(t)$ is the adopted law of star formation. The third model of interest, the 1-Gyr Burst model, therefore corresponds to $\mu = 1$ (although Bruzual termed it the C-model). The burst model is important because it represents the simplest null hypothesis for galaxy formation and evolution, i.e. a single epoch of star formation followed by only passive stellar evolution thereafter. This model can also be used to construct models of galaxy evolution involving a series of distinct starbursts etc. Finally, to avoid confusion, we emphasize that *both* the UV-hot and UV-Cold models used in the present study have exponential laws of star formation, because an alternative UV-Hot model has now been proposed by Rocca-Volmerange (1989), in which the star-formation rate is proportional to the gas density (this revised UV-Hot model provides improved fits to the UV-optical spectra of M87 and NGC4645).

Since the subsequent analysis of the radio-galaxy photometry centres on the comparison of the data with these three alternative models of elliptical galaxy evolution, samples of the evolving stellar spectra are shown in Fig. 1. The Burst, UV-Cold and UV-Hot models are illustrated in Fig. 1(a, b and c, respectively). In each case the synthetic spectrum is shown at three different times in the life of the galaxy, 0.5, 3.5 and 15.5 Gyr after the epoch of galaxy formation. The flux units are 5.32×10^{22} W Å^{-1} $M_{\odot}^{-1}$ (the synthetic spectra are published in more detail in Rocca-Volmerange & Guiderdoni 1988). These figures demonstrate clearly the important differences between the three alternative models. The Burst model, because it possesses the largest initial burst of star formation, begins life as the brightest of the three models, but decays rapidly in the UV thereafter. The UV-Cold model starts out slightly less spectacularly, but maintains significant UV flux at later times because the exponentially decaying law of star formation results in young massive stars still arriving on the main sequence after the initial epoch of formation. However, by $t_{\rm gal} \sim 10$ Gyr the flux shortward of 2000 Å has decayed essentially to zero. Finally, the UV-Hot model, with its more gently declining exponential law of star formation, begins even less spectacularly, but is still displaying enough star-formation activity after 13 Gyr to simulate the largest UV-excess seen in elliptical galaxies today.

All three models clearly show the evolution of the 4000-Å break with time, and also the increase in 1-μm flux at late epochs which is caused by the development of the Giant Branch. This latter effect is more pronounced in the Burst and UV-Cold models than in the UV-Hot one, because larger fractions of the stellar population are well evolved.

2.4 THE SYNTHESIS OF COLOUR EVOLUTION FROM THE EVOLVING SPECTRA

This section describes the details of how tracks of apparent magnitude and colour evolution, suitable for direct comparison with the data, were constructed from the library of evolving model spectra.

In the present study, the B and R photometry of the radio identifications was obtained through Kitt Peak Mould interference filters, while the observations at K were made through

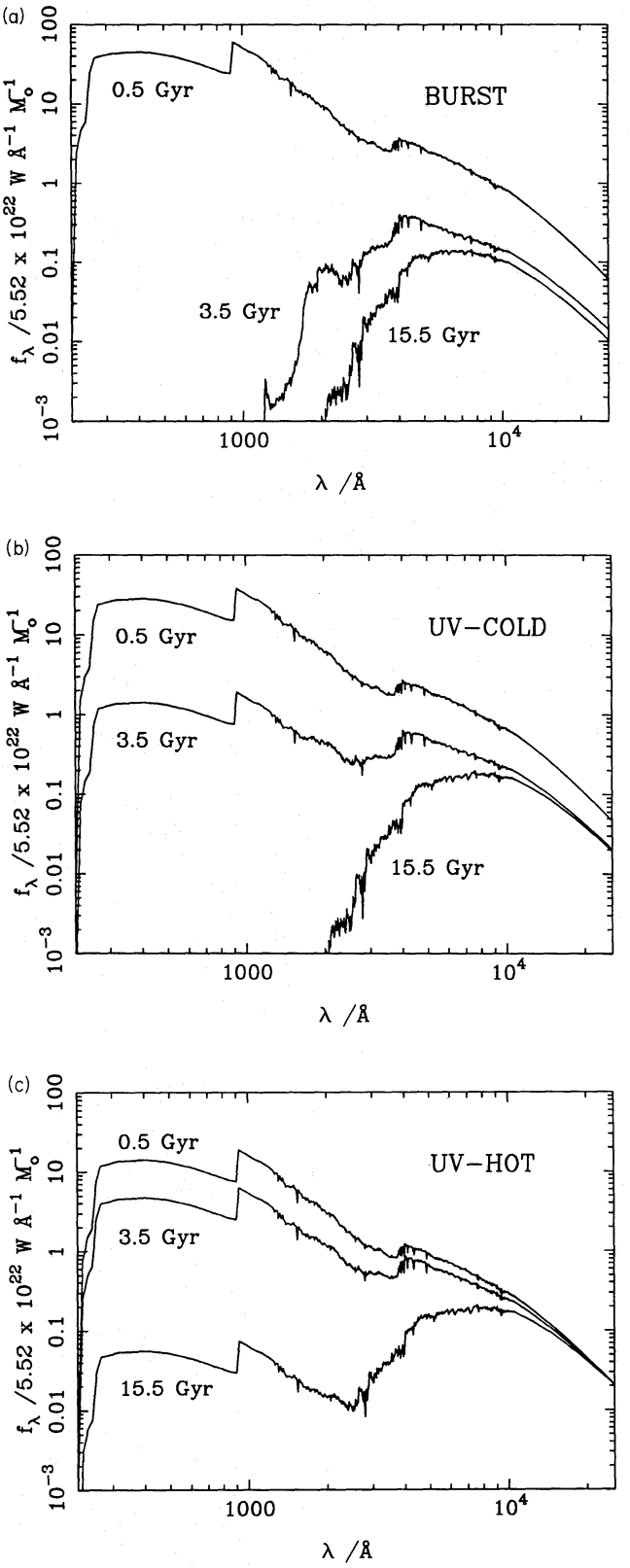

Figure 1. The time evolution of the model elliptical galaxy spectra. For each model, the form of the spectrum is shown at three different epochs in the life of the galaxy – 0.5, 3.5 and 15.5 Gyr after formation. (a) The Burst model; (b) The UV-Cold model; (c) The UV-Hot model.

the UKIRT K filter (see Dunlop *et al.* 1989). The response profiles of these three filters were obtained at ~25 Å resolution (courtesy of C. R. Benn, RGO). The B and R filter profiles were then multiplied by the spectral response of the RCA CCD which had been used to make the observations at the AAT – the fact that some of the R photometry was obtained using a TI CCD at the University of Hawaii 88-inch telescope is not a problem since the spectral responses of the two CCDs are in fact very similar (both chips are thinned and back-illuminated). Fig. 2 shows the response profiles of the three filters (B, R and K), including the impact of the spectral response of the RCA on the B and R profiles – the main effect is the degradation of the blue wing of the B filter.

The integrated broad-band fluxes were converted into magnitudes using a flux-calibrated spectrum of Vega which was constructed from the optical calibration of Hayes & Latham (1975) and the infrared measurements of Mountain *et al.* (1985). The effect of wavelength-dependent atmospheric extinction was also incorporated into the calculation, although this was found to have a negligible effect on the computed magnitudes. The evolving model galaxy spectra were then interpolated from the original $t=1$ Gyr to $t=0.1$ Gyr sampling; each point was then associated with a redshift z, cosmological look-back time τ, and effective distance D, the values of which were dictated by the choice of cosmology (i.e. density parameter Ω_0 and Hubble's constant H_0) and the assumed redshift of galaxy formation z_f. Then, at each evolutionary step, the broad-band integration was carried out after the appropriate redshifting and dimming of the model-galaxy spectrum. The absolute normalization of the resulting apparent magnitudes was determined by comparison with the magnitudes of the low-redshift radio galaxies in the sample.

3 Data

3.1 SELECTION OF THE GALAXY SAMPLE

For comparison with the models of spectral evolution described above, a galaxy subsample was selected from the complete, 178-source Selected Regions radio sample (Dunlop *et al.* 1989).

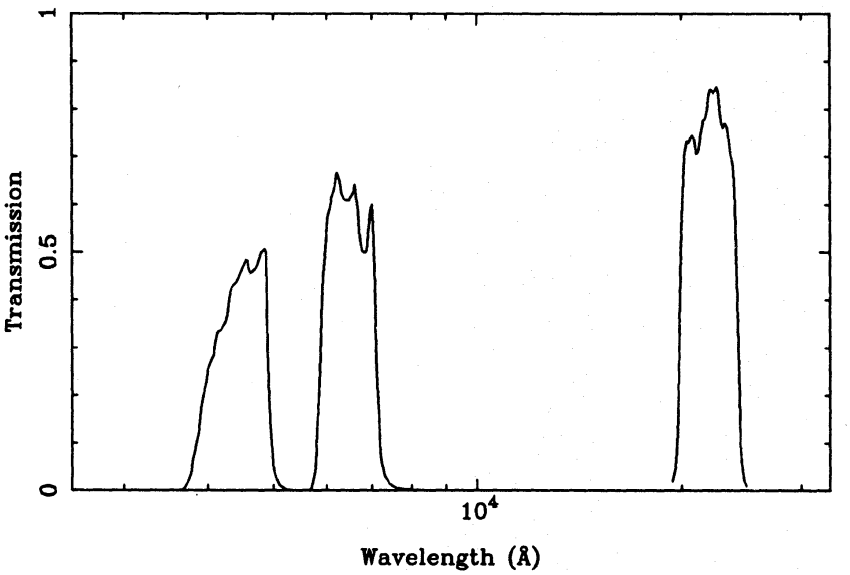

Figure 2. The broad-band filter profiles used to simulate evolution of apparent magnitudes and colours from the model spectra. The figure shows the 'effctive' Kitt Peak Mould B and R interference filter profiles (incorporating the spectral response of the RCA CCD) and the UKIRT K-filter profile.

First, in order that a reasonably complete three-colour dataset could be constructed, attention was confined to the four regions (out of six) for which 'complete' K photometry had been obtained (i.e. the regions centred on 0^h, 1^h, 2^h and 22^h – see Dunlop *et al.* 1989). The galaxy subsample was then selected to consist of all sources in these four regions which were classified as G or G? and which possessed a measured K magnitude. As discussed in Dunlop *et al.* (1989), the fraction of faint galaxies in this four-region subsample which lack K photometry is very small (six out of 70), and so the galaxy subsample thus selected may be regarded as complete.

One drawback of the resulting galaxy sample is that it contains very few sources with measured redshifts, despite the fact that the redshift content of the Selected Regions sample as a whole is now approaching 50 per cent (the bulk of the objects with spectroscopically determined redshifts are quasars and bright galaxies). Thus, for most of the faint galaxies of interest in the present study, redshifts have to be estimated and the most reliable method is to use the empirical K–z relation for radio galaxies (see Dunlop *et al.* 1989; Lilly & Longair 1984). All the galaxies in the present subsample have measured K magnitudes, and so we were able to use the K–z relation to estimate all of the missing redshifts. The relation used is the empirical one given by Lilly *et al.* (1985): $\log_{10} z = -5.368 + 0.384K - 0.00385K^2$, which is well defined out to $z \sim 1.7$. The problems of extrapolating the K–z relation to larger redshifts, and the sensitivity of the results to errors in redshift estimation are discussed in Section 4.4. However, it is important to stress that most of the important conclusions of this study result from the colours of galaxies at $z \sim 1$, for which the redshift estimates are reasonably secure.

3.2 APERTURE CORRECTIONS

The infrared measurements were made using apertures of diameter either 12.4 or 7.8 arcsec, while the CCD optical magnitudes were all measured through a 5-arcsec aperture after deconvolution of the seeing profile (see Dunlop *et al.* 1989). We considered it desirable to avoid any complex and subjective alteration of the raw photometry, but at the same time it was important to consider whether any simple corrections could be applied to improve the homogeneity of the data.

It was decided not to apply any aperture corrections to the infrared data. Since essentially all of the sky-survey identifications were observed through the 12.4-arcsec aperture, the mixed aperture IR data are confined to the fainter CCD identifications. The bulk of these CCD identifications are faint galaxies, most of which should be sufficiently distant ($z \sim 1$) for effectively all their light to be contained within a 7.8-arcsec aperture, and so no aperture correction is justified.

The CCD optical photometry is internally homogeneous (i.e. all 5-arcsec seeing-deconvolved aperture magnitudes). It therefore only remained for us to consider whether any correction should be applied to the optical photometry to assist comparison with the infrared data. For this purpose it was decided to correct all the galaxy 5-arcsec aperture magnitudes to a 7.8-arcsec aperture since, even at $z \sim 2$, the light of a giant elliptical galaxy is not expected to be fully contained within a 5-arcsec aperture (extrapolation to even larger apertures was considered a dangerously large modification of the raw data and, in any case, is not justified for the distant galaxies – see above). This correction can be made uniform and simple, involving merely the application of a constant offset to the CCD magnitudes given by Dunlop *et al.* (1989).

The only assumption involved in this aperture correction is the Structure Parameter, α, introduced by Gunn & Oke (1975), where $L \propto R^\alpha$. α is itself a function of R and it is common (e.g. Gunn & Oke 1975; Lilly, McLean & Longair 1984) to consider a sampling radius of 19.2

h_{50}^{-1} kpc, where $H_0 = h_{50} \times 50$ km s^{-1} Mpc^{-1}. At $z \sim 1$ (which should be a reasonable approximation for the faint CCD galaxy identifications) an aperture radius of 2.5 arcsec corresponds to a metric radius of ~ 20 kpc (for $H_0 = 50$ km s^{-1} Mpc^{-1}, $\Omega = 1$) and so it is reasonable to use the quoted values of α to correct the 5-arcsec diameter aperture magnitudes in the present study. The value of α adopted here was 0.5. This represents a compromise between the value of 0.7 found by Schneider, Gunn & Hoessel (1983) for Abell cluster galaxies, and the lower value of 0.4 found by Lilly *et al.* (1984) for 3C radio galaxies (because α is <1, the exact value is not too important for the present study). With this assumed brightness distribution, the aperture correction from 5 to 7.8 arcsec is $\Delta m = -0.24$. This offset was therefore applied to the results of the CCD galaxy photometry prior to the subsequent analysis.

Without more detailed information concerning the surface brightness distributions and redshifts of the galaxy identifications, no more complex procedure than the above is justified. This simple correction should assist in achieving the important aim of meaningful optical–infrared colours for the high-redshift galaxies (and the size of this correction gives an idea of the size of possible systematics in the optical–infrared colours).

3.3 EXCLUSION OF COMPACT RADIO SOURCES FROM THE SAMPLE

It remained for us to consider whether the galaxies associated with compact radio sources should be rejected from the sample because the colours of these objects might be influenced by the presence of a non-thermal component. The data are illustrated in Fig. 3 in the form of plots of optical–infrared R–K and optical B–R colour versus redshift (measured, or estimated from the K–z relation – see Section 3.1). Galaxies associated with extended double radio sources are shown as filled circles, those associated with compact sources (U or P in Downes *et al.* 1986) as open circles. There are 66 galaxies in the sample, but six of these (0003+006, 0017+026, 0105+025, 0225+002, 2158−170, 2357−006) are not present on the B–R/z diagram, either because of lack of B photometry, or because B and R magnitudes are lower limits (i.e. optical empty fields which were detected in the infrared). The large error bars at low redshift belong to those galaxies for which only eye-estimated optical magnitudes from Schmidt plates have been obtained. For $z < 0.1$, such objects have been omitted from the $(R$–$K)/z$ diagram because the systematic error in R–K is comparable with the error in the eye-estimated R magnitude (at such low z the extent of the galaxy visible on Schmidt plate is significantly larger than the 12.4-arcsec aperture used for the K photometry). Finally, to improve clarity the redshift scale in Fig. 3 has been restricted to $z \leqslant 3$, which results in the omission of one object (2204−182) with an estimated redshift of $z = 3.45$.

It is clear from Fig. 3 that three of the most obvious outlying datapoints are compact sources – two compact galaxies (2159−215 at $z = 2.2$, and 2207−203 at $z = 1.4$) have very blue optical–infrared colours but very red optical colours, while one compact galaxy (0055+015 at $z = 0.679$) is very red in R–K but very blue in B–R. These three sources are therefore obvious candidates for non-thermal contamination. in general the other compact sources lie in regions of the diagram which are also occupied by extended sources, particularly in R–K. However, in the B–R diagram there appears to be a trend for the compact sources to be rather blue at low redshift, and rather red at high redshift (particularly considering that many of the B–R colours at $z \sim 1.3$ are lower limits). In other words, the B–R colour of these sources seems approximately independent of z, suggestive of a power-law spectrum. For consistency it was therefore decided to remove all the compact sources (U and P radio structures) from the galaxy sample. The sample used throughout the remainder of this paper thus consists of 50 galaxies (46 with B–R information), all of which are the hosts of extended double radio sources. This should help to ensure that the observed colours genuinely reflect the stellar

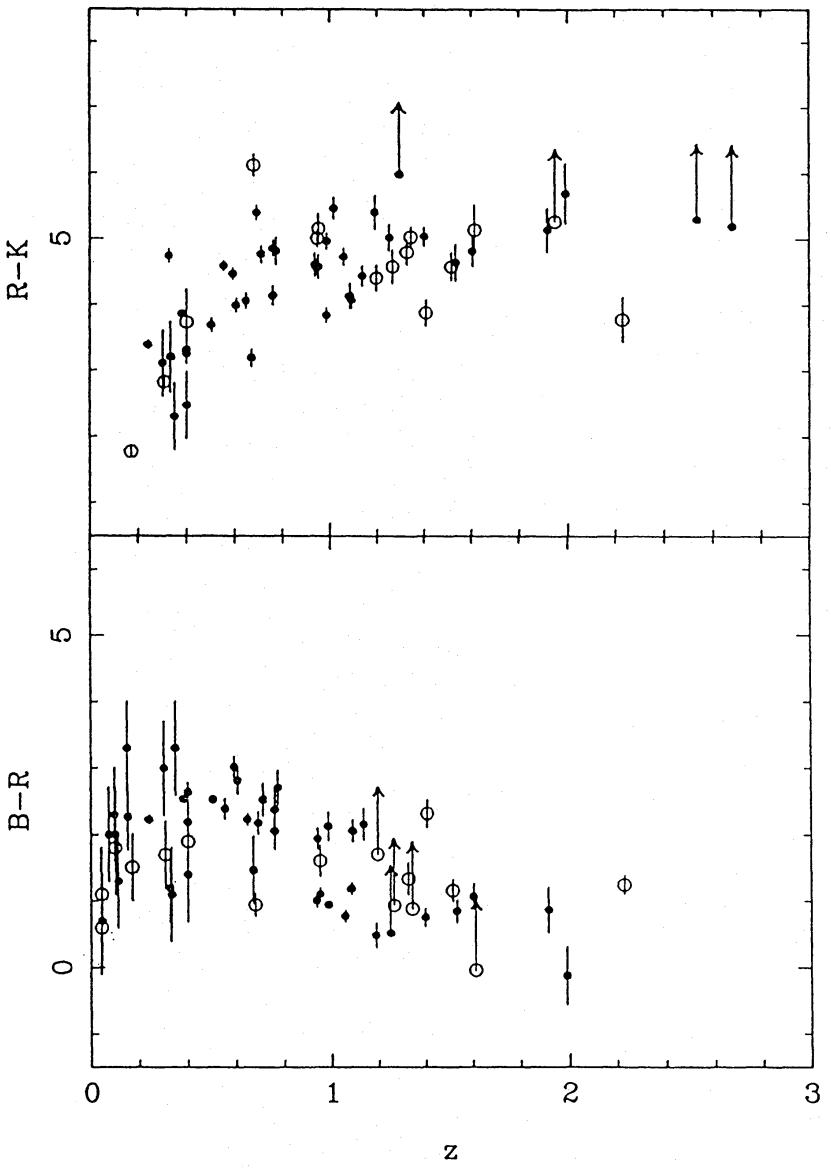

Figure 3. The optical–infrared (R–K) and optical (B–R) colour versus redshift diagrams for galaxies in the four-region subsample of the Selected Regions. Galaxies associated with extended sources are shown as filled circles, those associated with compact sources as open circles.

populations of the galaxies, and also enables direct comparison with the results of the earlier work on low-frequency radio samples (e.g. Lilly & Longair 1984).

4 Comparison of models and data

The results of the comparison of the models and the data are presented in this section in the form of plots of optical–infrared (R–K) and optical (B–R) colour versus redshift. This is a particularly instructive approach, since it facilitates simultaneous study of both the old and young stellar populations in the galaxies. It is also the best way to analyse the photometric data, given that the fraction of estimated redshifts is so large – the interpretation of colour evolution is less sensitive to exact values of z than is the analysis of Hubble diagrams. A further advantage of colour-redshift diagrams is that they are less affected by aperture and seeing

corrections and possible luminosity selection effects than are diagrams of apparent magnitude versus z.

The data which appear on the following plots are the same as in Fig. 3, except for the exclusion of the compact radio sources (see Section 3.3).

4.1 EVIDENCE FOR EVOLUTION

The obvious first question to address is whether all the radio galaxies in the sample exhibit spectral evolution. The null hypothesis of no evolution (NE) can be easily checked by simply redshifting (i.e. K-correcting) the present-day UV-Cold and UV-Hot elliptical spectra (i.e. the 13-Gyr end-points of the UV-Cold and UV-Hot models). Since these two spectra are known to bracket the observed range of UV spectra observed in nearby ellipticals, the corresponding K-corrections should map out the locus of possible colour-redshift tracks which could be regarded as consistent with zero evolution. The UV-Cold and UV-Hot NE tracks are shown in Fig. 4. The important conclusion to be drawn from this figure is that *all* the rdio galaxies show significant colour evolution above $z \sim 0.6$. It is important to note, however, that it is the $R-K$ diagram which establishes this result, and that no such conclusion could have been reached solely on the basis of the optical data. On the $R-K$ diagram *both* UV-Cold and UV-Hot NE models are too red to fit the upper envelope of the data above $z \sim 0.6$, thus demonstrating that all the galaxies in the sample display some evolution beyond this redshift. In contrast, on the $B-R$ diagram, although the UV-Cold NE model is clearly too red at $z \sim 0.6$, the UV-Hot NE model provides a reasonable description of the data at all epochs, and from this diagram it could only be concluded that a subset of galaxies (i.e. those bluer than the UV-Hot NE model) display evolution. This feature of the $B-R$ diagram is consistent with the conclusions of other workers who have considered only optical data – in his review of spectral evolution, Bruzual (1985) states that 'the only safe conclusion that has been established is that some distant galaxies are brigher in the UV than most nearby elliptical galaxies'. The problem with the optical data is that any conclusion concerning the existence of evolution depends on what is taken as the present-day UV spectrum – it is clear from Fig. 4 that the UV colours of a large fraction of the galaxies in the sample can be adequately described, at all epochs, by the extreme UV-Hot spectrum observed in ellipticals today. In contrast, at least up to $z \sim 1$, the K-corrections in $R-K$ are relatively unaffected by the chosen level of present-day far-UV light.

The superior ability of the $R-K$ diagram to demonstrate unambiguously the presence of at least passive evolution was first demonstrated by Lilly & Longair (1984). They showed that the upper envelope of the $R-K$ colours of the 3C radio galaxies was inconsistent with an NE model. However, they only considered a single elliptical galaxy template spectrum, whereas Fig. 4 demonstrates the existence of evolution using NE models which cover the observed range of present-day elliptical spectra.

4.2 MODELLING THE COLOUR EVOLUTION OF THE RADIO GALAXIES

4.2.1 The conflict between the R–K *and* B–R *colour diagrams*

When an attempt is made to describe simultaneously the $R-K/z$ and $B-R/z$ data by a simple model of galaxy evolution, it is found that the two colour diagrams tend to fight against each other. This feature is illustrated in Fig. 5. In this figure the data are compared with the colour evolution tracks produced by the UV-Cold ($\mu \sim 0.6$) and UV-Hot ($\mu \sim 0.3$) evolving models, assuming $\Omega_0 = 0$, $H_0 = 50$ km s^{-1} Mpc^{-1}, and a formation redshift of $z_f = 5$. It is seen that the two models bracket nicely the locus of points on the $B-R/z$ diagram, but that the same two

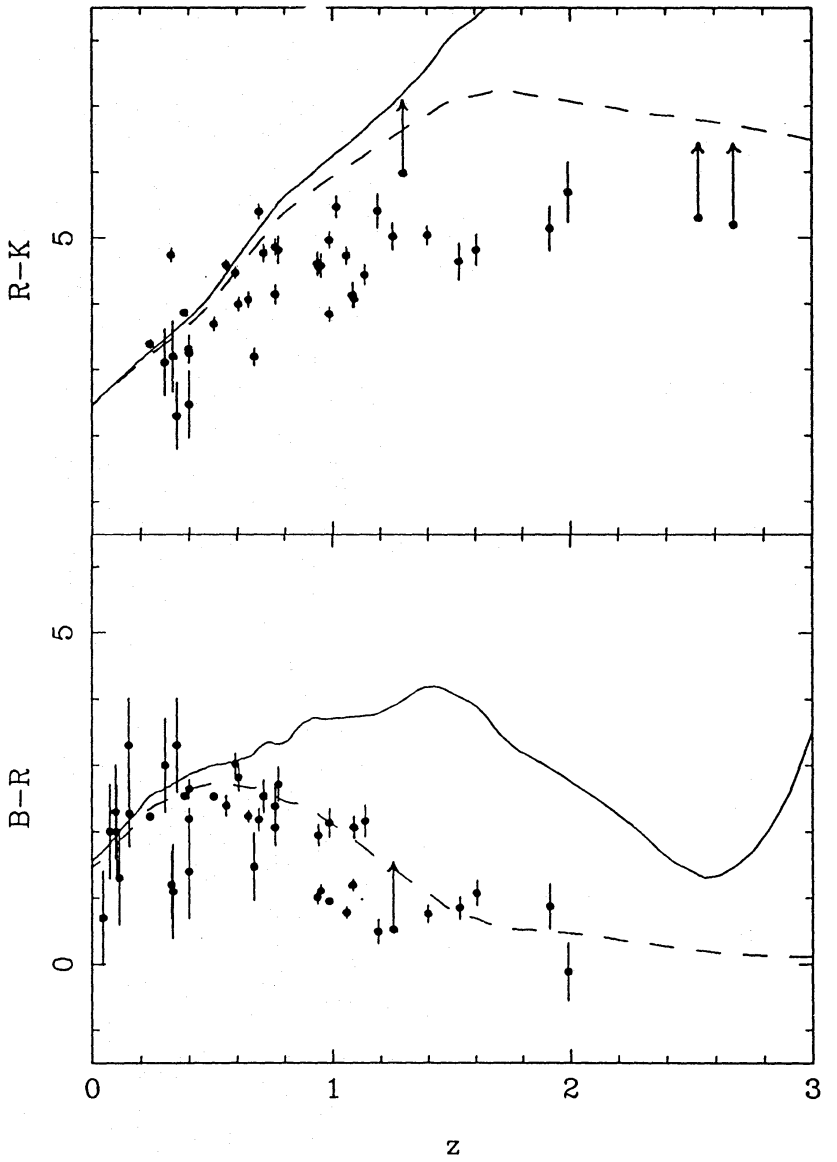

Figure 4. The $R-K$ and $B-R$ colour versus redshift diagrams showing the data compared to the colour evolution tracks produced by simply redshifting the present-day UV-Cold (solid line) and UV-Hot (dashed line) elliptical spectra.

models are completely unable to describe the $R-K/z$ data. Older models with weaker evolution – either higher values of μ, or larger formation-redshifts – are needed to fit the optical–infrared colours. Spinrad & Djorgovski (1987) noted similar behaviour in a comparison of the colours of 3C radio galaxies with the models of Bruzual, 'the data in the visual regime indicate the more active models, $\mu \sim 0.6$ but the data in the near-IR are consistent with the quieter models, $\mu \sim 0.8$ or even the passive C-models'. Spinrad conjectures that this may indicate some problem with the models. It is interesting that the same behaviour is found in the present study using both new models and a new independent set of data (although the two models have many features in common). It is also interesting to note the similarity of the model which fits the upper envelope of the $B-R$ data in Fig. 5, with the Bruzual model which describes the upper envelope of the optical colours of the 3C galaxies – a $\mu = 0.7$ Bruzual model with $\Omega_0 = 0$, $H_0 = 50$ km s^{-1} Mpc^{-1}, and $z_f = 5$ is shown by Spinrad (1986) as providing a good description of the upper envelope of the $V-R$ colours of the 3C galaxies.

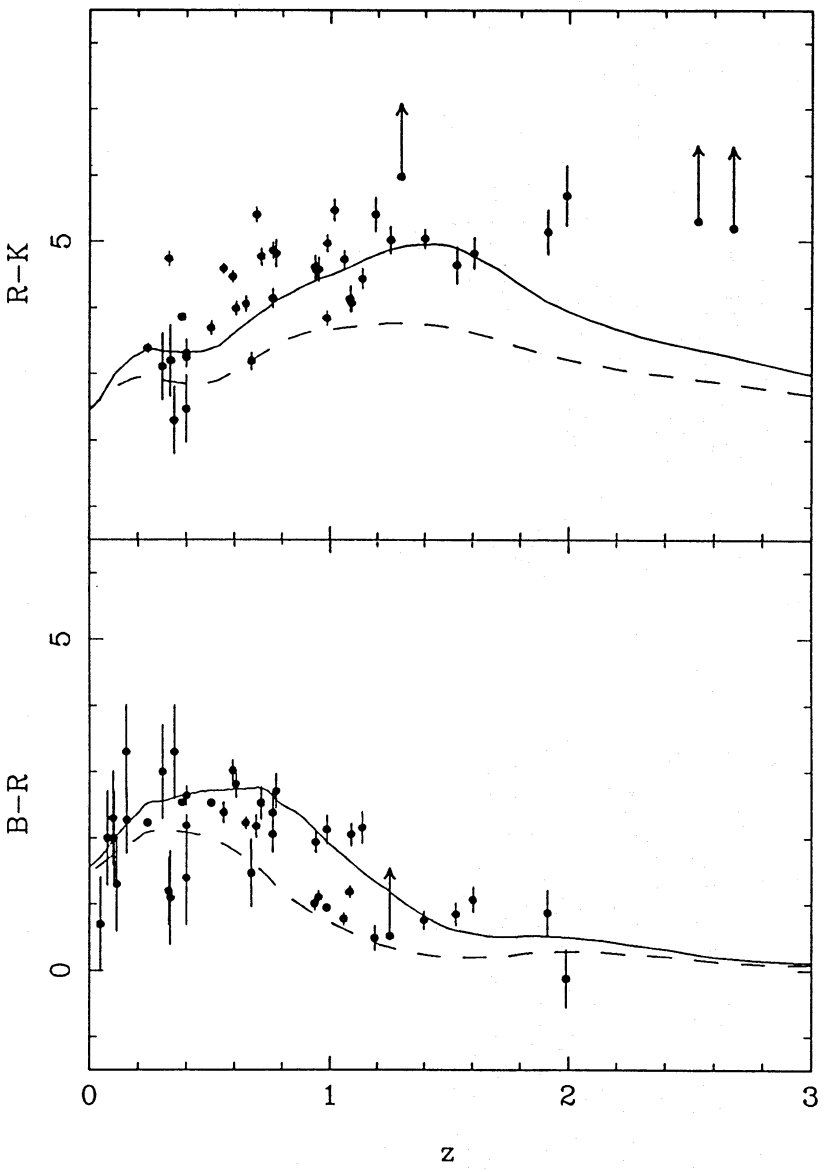

Figure 5. Comparison of the data with the $R-K$ and $B-R$ colour evolution of the UV-Cold (solid line) and UV-Hot (dashed line) models, assuming $\Omega_0 = 0$, $H_0 = 50$ km s^{-1} Mpc^{-1} and formation redshift $z_f = 5$.

4.2.2 Modelling the red envelope

As mentioned above, older stellar populations are needed in order to produce redder colours. In principle, therefore, the red envelope on the $R-K/z$ diagram should represent the oldest galaxies in the sample and, however the blueward scatter from this envelope is to be interpreted (e.g. varying levels of star-forming activity or a range of formation reshifts – see Section 4.3), it is important to find a model which is consistent with these oldest, relatively passive objects. The conflict between the two colour diagrams described above means that such a model is unlikely to be able also to describe the upper envelope in $B-R$, but, since the infrared photometry samples the oldest stellar populations in the galaxy, it is important to try to fit the envelope in the $R-K$ diagram first –models consistent with both diagrams are discussed below. In Fig. 6 the $R-K$ colour evolution of the Burst and UV-Cold galaxy models is shown for a range of galaxy formation redshifts, $z_f = 3$, 5, 10 and 20. $\Omega_0 = 0$ and $H_0 = 50$ km s^{-1} Mpc^{-1} are

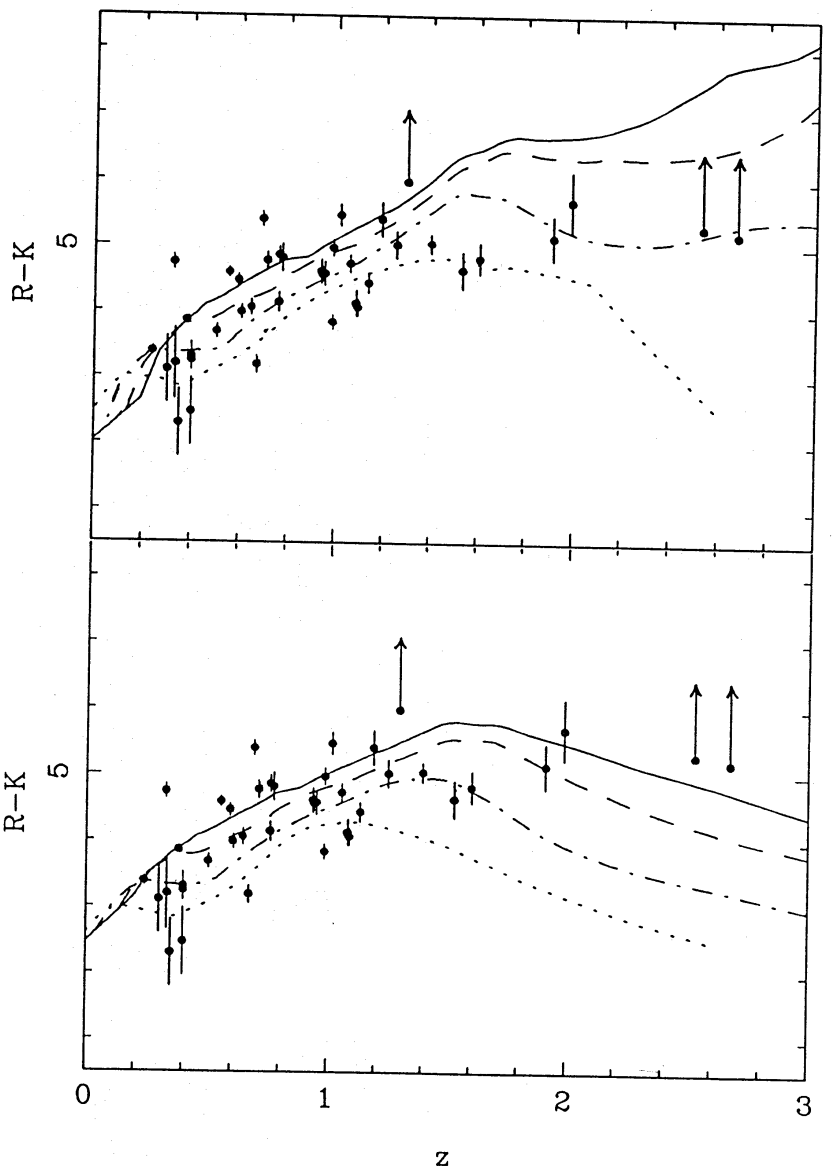

Figure 6. The effect of varying the formation redshift of the Burst (upper diagram) and UV-Cold (lower diagram) models in an attempt to produce old-enough models to fit the red envelope of the R–K data. $\Omega_0 = 0$ and $H_0 = 50$ km s^{-1} Mpc^{-1} are assumed and formation redshifts of $z_f = 3$ (dotted), 5 (dot-dash), 10 (dashed) and 20 (solid) are shown.

assumed. This figure shows that, even with these relatively inactive models, it is a struggle to reproduce the reddest observed galaxy colours at $z \sim 1$. It is only really achieved with the very oldest models shown – i.e. $z_f = 20$, which corresponds to a galaxy age $t_{gal} \sim 18$ Gyr – and even then there are a few unexplained very red points. The corresponding plots for $\Omega_0 = 1$ are shown in Fig. 7. In a critical Universe, a fit to the red envelope in R–K cannot be achieved unless a very low value for the Hubble constant is assumed, because the Universe is simply not old enough. A similar problem has been encountered by other workers in trying to fit Bruzual's models to the red envelope of their colour data – Windhorst, Koo & Spinrad (1986) derive ages of 14–16 Gyr for the oldest galaxies in their millijansky sample from attempts to fit Bruzual's models to the red envelope of the optical (J–F) colour redshift diagram. The work of Hamilton (1985) on the 4000-Å break also implies large ages – he has found galaxies at $z \sim 0.8$

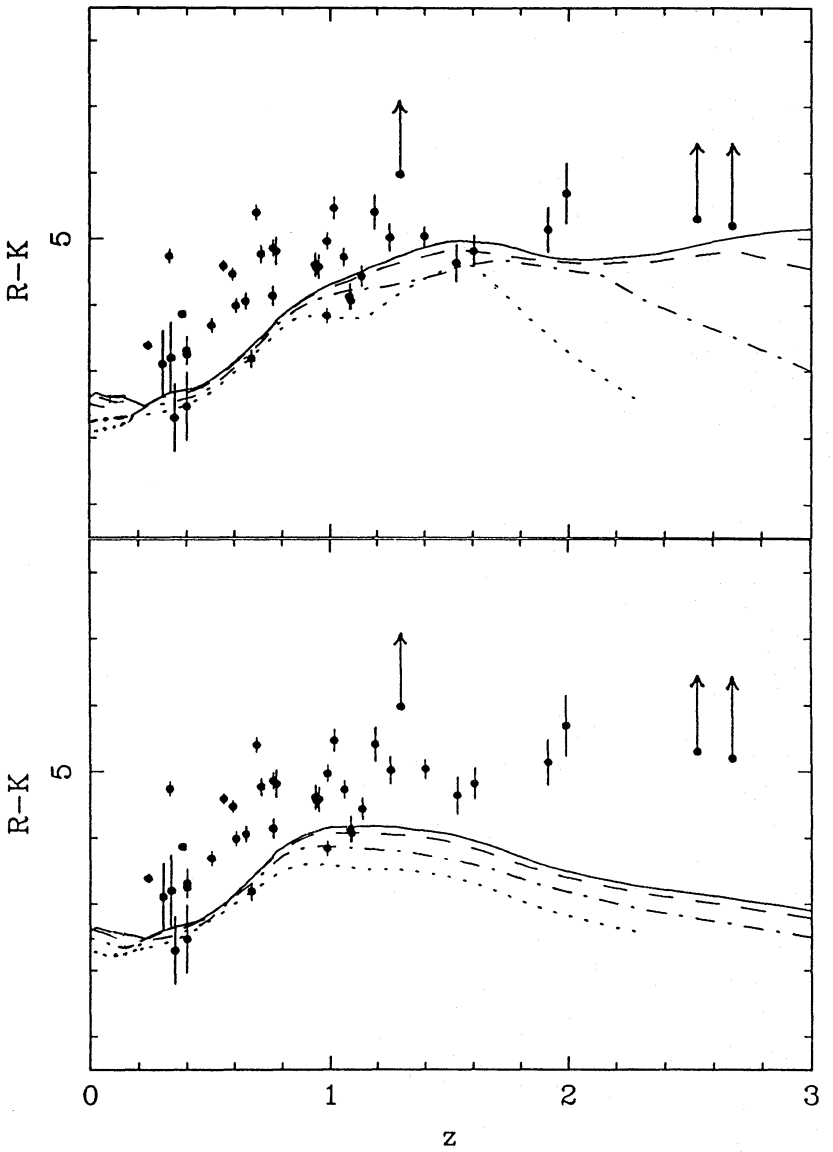

Figure 7. The same as the Fig. 6, but this time assuming a critical Universe, $\Omega_0 = 1$. With $H_0 = 50$ km s^{-1} Mpc^{-1}, the critical Universe is not old enough to contain models that are sufficiently old to model the reddest *R–K* colours.

corresponding to a look-back time of $\tau = 8.6$ Gyr (assuming $\Omega_0 = 0$, $H_0 = 50$ km s^{-1} Mpc^{-1}) which are already 8–9 Gyr old based on the evolution of the 4000-Å break in Bruzual's models. The ages implied by the present study (i.e. ~18 Gyr) are comparable with or even slightly greater than the most extreme results quoted above, partly because they are based on optical–infrared colours, and partly because the new models do not produce such red colours at $z \sim 1$ as do Bruzual's. For ellipticals, the derived ages appear to be only weakly sensitive to the choice of IMF (Bruzual 1983a; Bruzual & Kron 1980) and, taken literally, the new results suggest $H_0 < 55$ km s^{-1} Mpc^{-1} ($\Omega_0 = 0$) and $H_0 < 35$ km s^{-1} Mpc^{-1} ($\Omega_0 = 1$). However, the age problem in the galaxy models is closely related to the well-known age problem for globular clusters; both arise from the same evolutionary tracks. Most recent studies of globular clusters (e.g. Gratton 1985; Ratcliff 1987) conclude that the ages of Galactic globular clusters are about or in excess of 15 Gyr. If low values of H_0 and Ω_0 are not desired, then some way of speeding up the stellar evolution models will have to be found.

4.2.3 Consistent models of minimum evolution

The absolute null hypothesis of zero evolution was rejected in Section 4.1. It is interesting, therefore, to consider what form of evolutionary model might fulfill the role of a new more realistic null hypothesis (in other words a model of minimum evolution). The requirement of such a model is that it should simultaneously be able to describe the red envelope in both $R-K$ and $B-R$ colour diagrams and therefore reproduce the colours of the least active galaxies in the sample.

Lilly & Longair (1984) showed that the passively evolving C-model was a reasonable null hypothesis model on the $R-K$ diagram for 3C radio galaxies. This is basically in agreement with Fig. 6 which indicates that on the $R-K$ diagram the Burst, and possibly also the UV-Cold model, produce reasonable tracks of minimum evolution, provided that they are old enough. In the present work, however, the null-hypothesis model must also describe the upper envelope of the $B-R$ data. In Fig. 8 the old ($z_f = 20$, $\Omega_0 = 0$, $H_0 = 50$ km s^{-1} Mpc^{-1}) Burst and UV-Cold models are illustrated on both $R-K$ and $B-R$ diagrams – it is clear that the old Burst model is not a reasonable null-hypothesis model in $B-R$. This result has already been hinted at above, and in a sense it is reassuring that a pure Burst model should be inadequate, given that it is incapable of reproducing the observed spectra of elliptical galaxies at the present day. The UV-Cold model in Fig. 8 is clearly a better model of minimum evolution, particularly in $B-R$, although it struggles to produce red enough $R-K$ colours at high z.

This combined analysis of the $R-K$ and $B-R$ colours therefore enables the following conclusions to be drawn:

(i) Based on the reddest $R-K$ colours, the initial epoch of star formation must be very early.

(ii) Based on the $B-R$ colours, all the galaxies in the sample must have undergone some degree of star-formation activity after the formation epoch of the oldest galaxies.

(iii) If conclusion (ii) were to be interpreted as a selection effect introduced by the fact that all the galaxies in the present study are radio sources, then this would imply an intimate, and probably direct connection between star-formation and radio-source activity (because it appears to apply to all the galaxies in the sample).

Of course there are various ways of modelling conclusion (ii). The UV-Cold model which gives an exponentially declining rate of star-formation is one. Another, and perhaps more promising possibility is to decouple the old and young stellar populations and consider a two-component model. Such a model is also shown in Fig. 8 (dotted line). This demonstrates the effect of adding to the old Burst model a constant small amount of UV flux at all epochs. The amount of UV flux which has been added is 0.7 × the UV flux (shortward of 3000 Å) of the present-day UV-Hot elliptical spectrum. It is clear from the figure that the addition of this small amount of UV flux, which is typical of that seen in at least some present-day ellipticals, is sufficient to enable the Burst model to fit the red envelope in the $B-R$ diagram without destroying its ability to produce very red colours in $R-K$. This composite model may therefore be regarded as an alternative null hypothesis of evolution to the UV-Cold model, and it seems that this sort of decoupling of the old and new stellar populations may well offer the best chance of reconciling the data at both optical and IR wavelengths (particularly since additional blueing in $B-R$ is much easier to explain than additional reddening in $R-K$ – see Section 4.3).

The 'Burst + UV light' model is of interest even if one rejects the view that the UV light in elliptical galaxies is produced by young stars. In this case the more conservative conclusion can still be stated that, by adding an amount of UV light commonly observed in present-day ellipticals (of origin not necessarily determined), an old Burst model can provide an adequate description of both the optical and IR data.

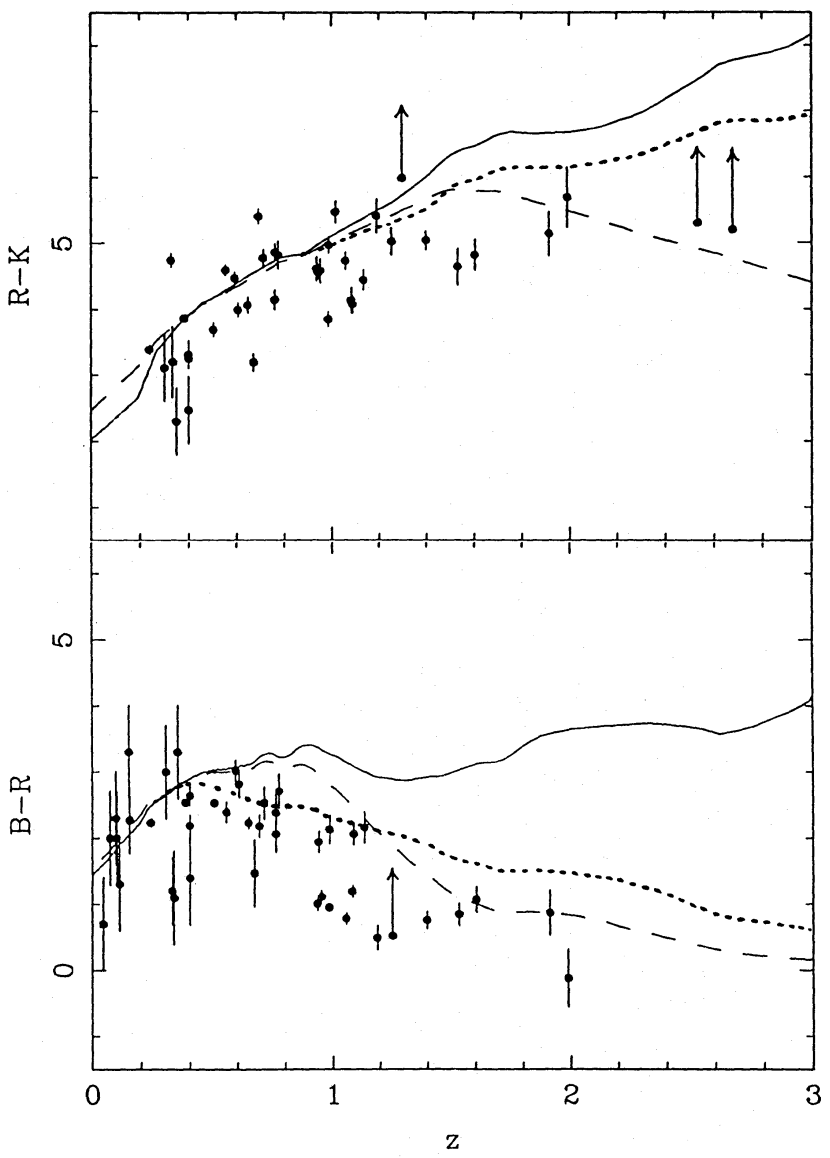

Figure 8. The $R-K$ and $B-R$ evolution of three alternative models of minimum evolution:

(i) Solid line – the oldest Burst model shown in Fig. 6 (i.e. $\Omega_0 = 0$, $H_0 = 50$ km s^{-1} Mpc^{-1}, $z_f = 20$). This model cannot fit the red envelope on both diagrams.

(ii) Dashed line – the oldest UV-Cold model shown in Fig. 6 (i.e. $\Omega_0 = 0$, $H_0 = 50$ km s^{-1} Mpc^{-1}, $z_f = 20$). This model is closer to fitting the red envelope in both diagrams, but struggles to reproduce the red $R-K$ colours at high z.

(iii) Dotted line – the old Burst model altered by the addition of a small and constant amount of UV flux at all epochs. The UV flux added consists of 0.7 × the UV spectrum shortward of 3000 Å which is observed in the present day UV-Hot spectrum. This small alteration is sufficient to make the burst model an acceptable model of minimum evolution in both diagrams.

4.3 THE ORIGIN OF THE BLUEWARD SCATTER

So far the discussion has been confined to the problem of finding models which are capable of describing the red envelope on both colour/redshift diagrams. It therefore still remains to consider the possible origins of the blueward scatter which is so apparent in both $R-K$ and $B-R$. In practice, the situation is probably very complex, and a detailed study of each individual galaxy could be necessary before a definite answer is possible. However, it is

interesting to consider two very different, and probably naïvely simplistic, ways in which the blueward scatter might arise.

The first extreme possibility is that all galaxies evolve in the same way, as indicated by the form of evolution required to fit the red envelope, and that the blueward scatter simply results from a range of formation redshifts. This possibility is investigated in Fig. 9, which shows the effect of varying the formation redshift of the two 'successful' models of minimum evolution which were discussed in the previous section. Fig. 9(a) shows the colour evolution of the UV-Cold model for a range of formation redshifts, $z_f = 1$, 2, 4 and 20, assuming $\Omega_0 = 0$, and $H_0 = 50$ km s^{-1} Mpc^{-1}. Fig. 9(b) shows the analogous plots for the Burst + UV model. These diagrams show that it is indeed possible to span the observed range of colours just by varying the formation epoch of these simple galaxy models. It is interesting that, in the case of the UV-Cold model (Fig. 9a), $z_f = 2$ is sufficiently recent to describe the bluest points at $z \sim 1$ in B–R, whereas the Burst + UV model requires these galaxies to be effectively newly formed. This means that, whatever the exact interpretation, some level of star formation at epochs later than $z \sim 2$ is required to reproduce the colours of the bluest galaxies in the sample. Taken literally, both models indicate that galaxy formation should continue up to $z \sim 2$, thus implying a large range of formation redshifts – $z_f = 20$ being required to model the reddest objects. It is worth remembering that this range does not seem so large when considered in terms of cosmological time – with $\Omega_0 = 0$ and $H_0 = 50$ km s^{-1} Mpc^{-1}, $z_f = 20$ corresponds to a look-back time of ~ 18.5 Gyr, while $z_f = 2$ corresponds to ~ 13 Gyr [Rocca-Volmerange (1988) has found similar ranges of z_f, however, for 3CR galaxies on the basis of Ly α fluxes].

These diagrams are deceptively impressive, however, if the R–K/z and B–R/z plots are viewed individually rather than together. Any viable model must explain the relative degrees of blueward scatter in B–R and R–K simultaneously for *each individual object*. Thus, objects which lie on a particular evolutionary track (for example the $z_f = 2$ track) in the B–R diagram should also lie on the corresponding track in R–K. This is certainly not the case for the Burst + UV model – the $z_f = 2$ track virtually follows the blue envelope in R–K but fails to reproduce the bluest B–R colours. For the UV-Cold model the two diagrams are rather more consistent, but the R–K colours still suggest rather higher formation-redshifts than are indicated by the optical colours. Nevertheless, as discussed below, it is relatively easy to account for some extra blueing in B–R by the addition of a small amount of recent star-formation activity, and so a range of z_fs may well be the correct explanation for the scatter in R–K (as well as much of the scatter in B–R).

The second extreme possibility is to assume that all the galaxies were formed at the same epoch, which must then, by necessity, be the epoch required to model the reddest galaxies (i.e. $z_f = 20$ for the present study). In this picture the blue scatter must then be considered to represent differences in the star-formation histories of individual galaxies. It is therefore interesting to consider the impact of sudden bursts of star-formation activity on the colour evolution of an old, otherwise passively evolving galaxy (i.e. an old Burst model). Models to investigate this effect were constructed by superimposing a second burst model on to an old $z_f = 20$ Burst model, after an appropriate delay in cosmological time. The two parameters of interest are clearly the size of the second burst relative to the size of the underlying galaxy, and the redshift at which it occurs. Fig. 10 illustrates the effect of varying the former. The redshift of the burst has been held constant at $z \sim 2$ (i.e. ~ 5.5 Gyr after formation of the underlying galaxy), while its size relative to the mass of the existing galaxy is varied from 1 (i.e. a merger) to 0.001. One interesting feature of this figure is that, immediately after the second burst has occurred, the B–R colour is very insensitive to the size of the starburst, whereas the amount of sudden blueing in R–K is a strong function of the fraction of mass involved. This behaviour is best understood by referring to Figs 1 and 2. The approximate centroid wavelengths of the B,

R and *K* filters are 4500, 6500 and 22 000 Å, respectively. At $z \sim 2$ these filters therefore sample the spectrum at rest-frame wavelengths of 1500, 2200 and 7300 Å. By this redshift, a Burst model formed at $z_f = 20$ is ~5.5-Gyr old and possesses very little flux shortward of ~3000 Å. As can be seen from the shape of the 0.5-Gyr spectrum in Fig. 1(a), the sudden occurrence of even a small burst will add a lot of ultraviolet flux to the spectrum of the galaxy and, because of the lack of residual flux from the old galaxy in this region, the resulting shape of the spectrum shortward of 3000 Å will be practically independent of the size of the new burst. It is thus clear why the *B*–*R* colour is independent of the size of the burst (at this redshift). In contrast to the situation in the ultraviolet, at 7300 Å the old galaxy produces a large flux, and so the addition of a small burst will have an insignificant effect on the measured

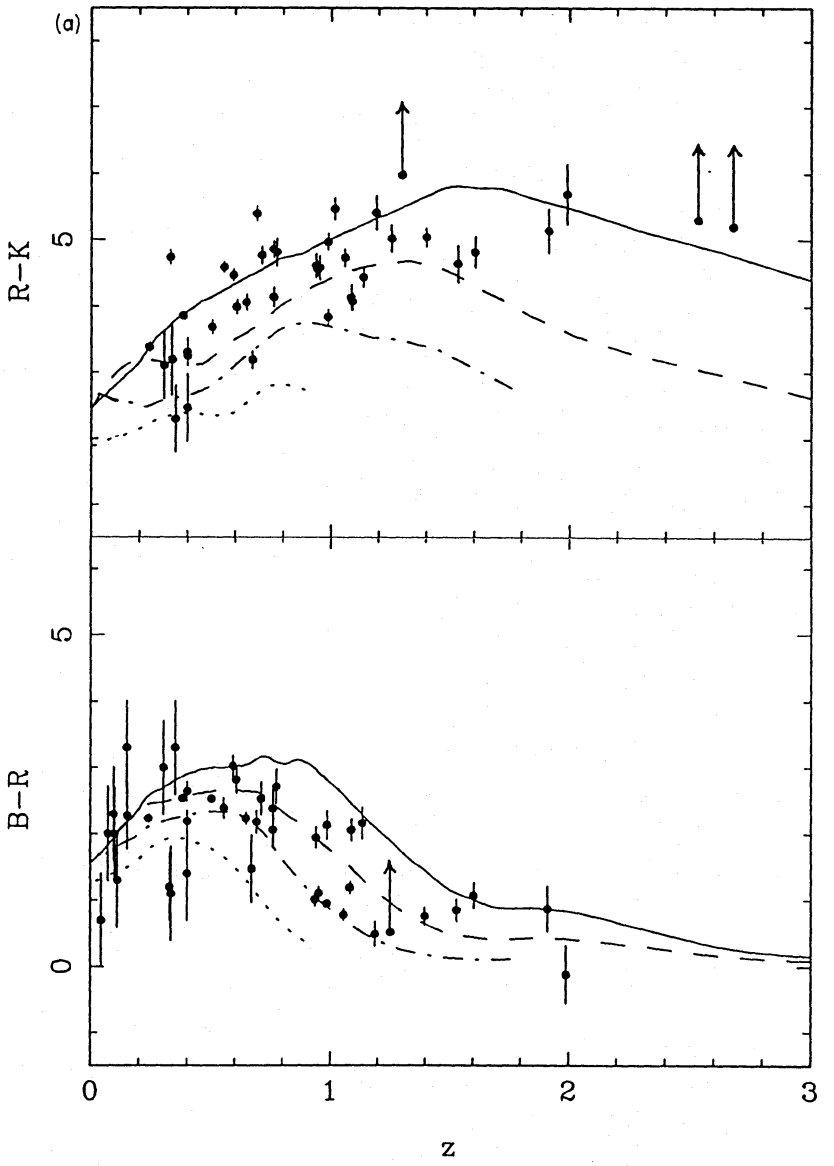

Figure 9. The effect on colour evolution of varying the redshift of formation. (a) The *R*–*K* and *B*–*R* colour evolution of the UV-Cold model for a range of formation redshifts, $z_f = 20$ (solid line), 4 (dashed line), 2 (dot-dash line), 1 (dotted line). $\Omega_0 = 0$ and $H_0 = 50$ km s^{-1} Mpc^{-1} are assumed. (b) The *R*–*K* and *B*–*R* colour evolution of the Burst + UV model (described in Section 4.2) for a range of formation redshifts, $z_f = 20$ (solid line), 4 (dashed line), 2 (dot-dash line), 1 (dotted line). $\Omega_0 = 0$ and $H_0 = 50$ km s^{-1} Mpc^{-1} are assumed.

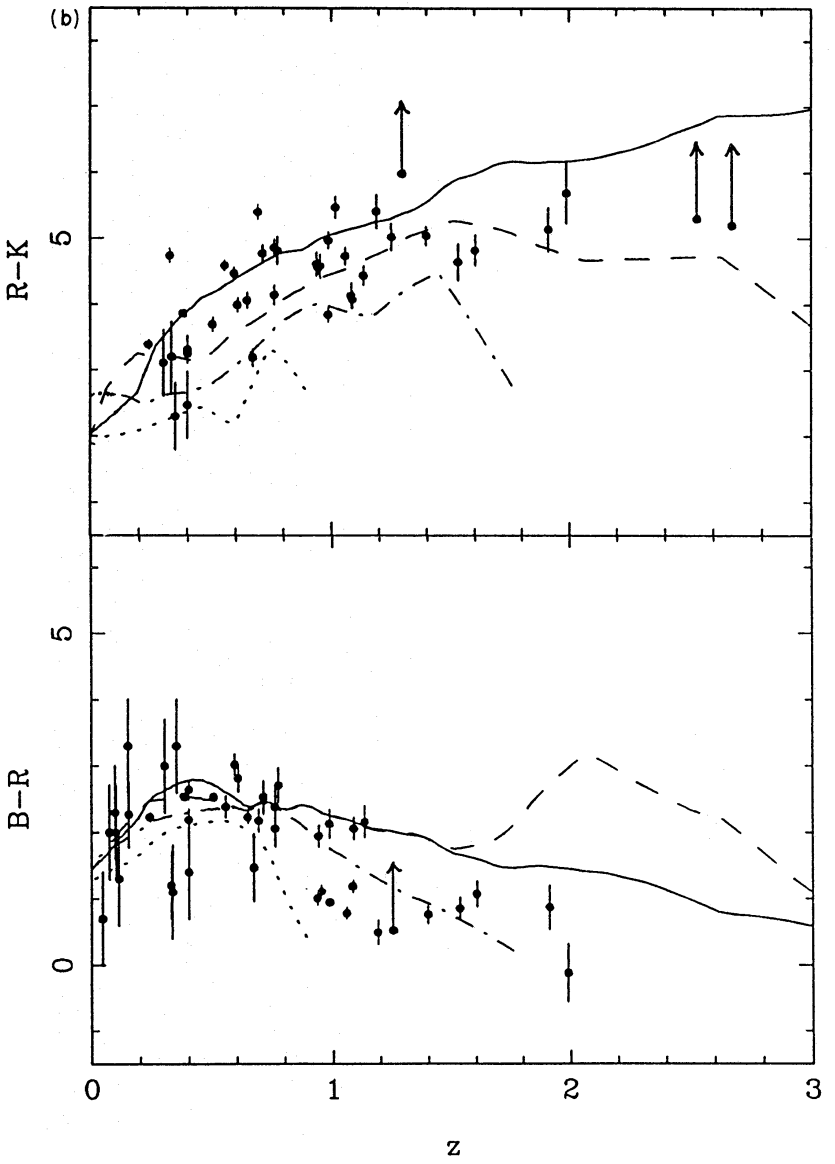

Figure 9 – *continued*

K magnitude. This makes the $R-K$ colour a very sensitive measure of the burst size because, at these high redshifts, the R filter is sampling the rest-frame ultraviolet light.

The $R-K$ colours can therefore be used to set limits on the permissible size of a starburst, relative to that of the underlying galaxy. If the two datapoints at $z \sim 2$ are to be explained by a starburst in an old galaxy, their $R-K$ colours constrain the size of that starburst to be ~ 0.01 $\times$ the mass of the galaxy (i.e. the dashed line in Fig. 10). It is then apparent from Fig. 10 that a starburst at $z \sim 2$ of this limited size does not affect the colours for very long. Indeed, even the largest burst shown, which represents a doubling of the size of the galaxy, cannot explain the bluest galaxies at $z \sim 1$ in either $R-K$ or $B-R$ diagrams.

This leads naturally on to the investigation of the second parameter – the epoch at which the second burst occurs. In Fig. 11 the burst size of $0.01 \times$ the galaxy mass has been taken as a working hypothesis, and the epoch of the burst has been varied –the figure shows the effects of starbursts occurring 5, 7 and 9 Gyr after the initial formation epoch (corresponding to redshifts of $z \sim 2$, 1.3 and 0.9). It is clear from the $B-R$ diagram that bursts of this magnitude

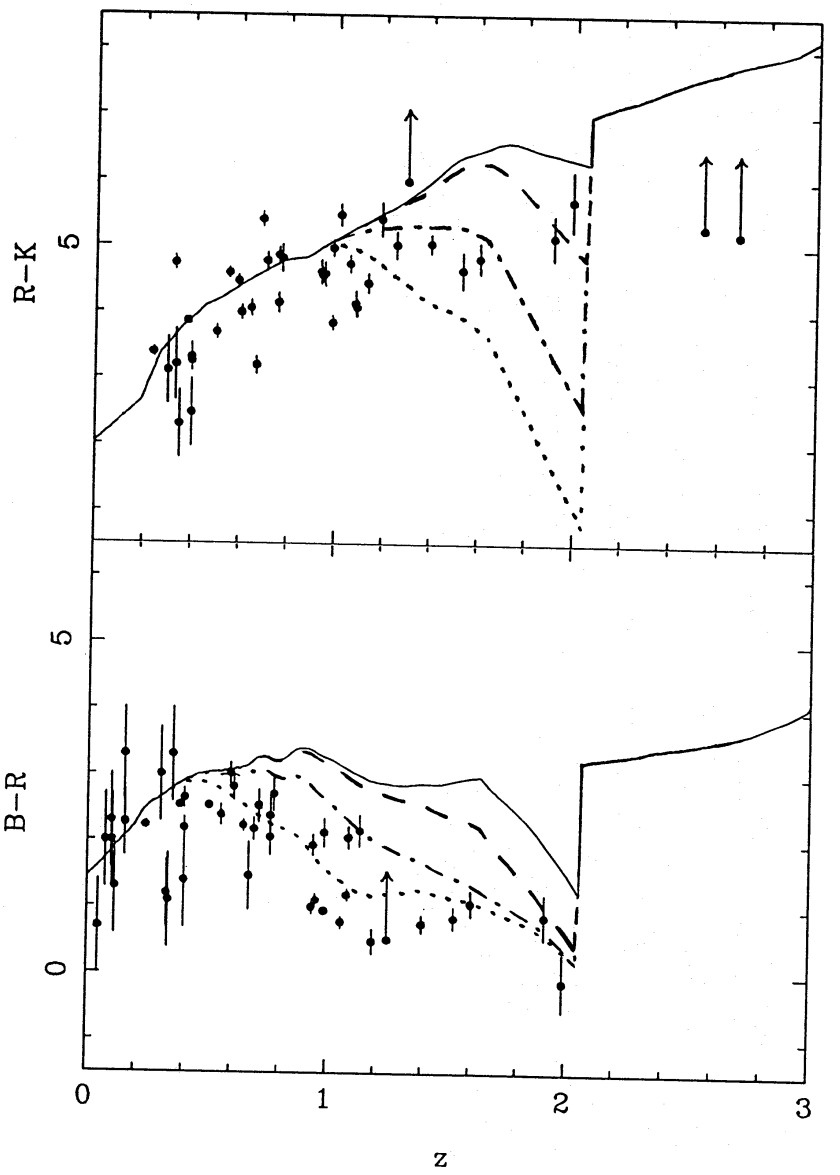

Figure 10. The effect on the R–K and B–R colour evolution of varying the size of a starburst which occurs at $z \sim 2$ in an old ($z_f = 20$) passively evolving elliptical galaxy. The fraction of the final galaxy which is assumed to form at $z = 2$ is 0.001 (solid line), 0.01 (dashed line), 0.1 (dot-dash line), 0.5 (dotted line). $\Omega_0 = 0$ and $H_0 = 50$ km s^{-1} Mpc^{-1} are assumed.

are sufficient to account for the full range of optical colours if a suitable burst redshift is chosen for each datapoint. This figure re-emphasizes the short recovery time from bursts of this size, implying that the optically bluest galaxies must be being observed at, or very shortly after, the occurrence of the starburst.

Small isolated bursts can therefore account for the blueward scatter in B–R, but it is clear from Fig. 11 that they do not succeed in R–K. For redshifts less than one, both the R and K magnitudes are relatively insensitive to the new UV flux from a small burst – a fact which is again best understood by referring to Figs 1 and 2 – so single small bursts cannot account for the scatter in R–K at low z. One way to reproduce the bluer R–K colours would be to increase the burst sizes sufficiently to affect the R magnitude at low z (despite the fact that the R–K colours of the few galaxies in the sample at $z \sim 2$ would seem more consistent with small bursts). Another solution is to build up the flux in the near-ultraviolet region via a series of

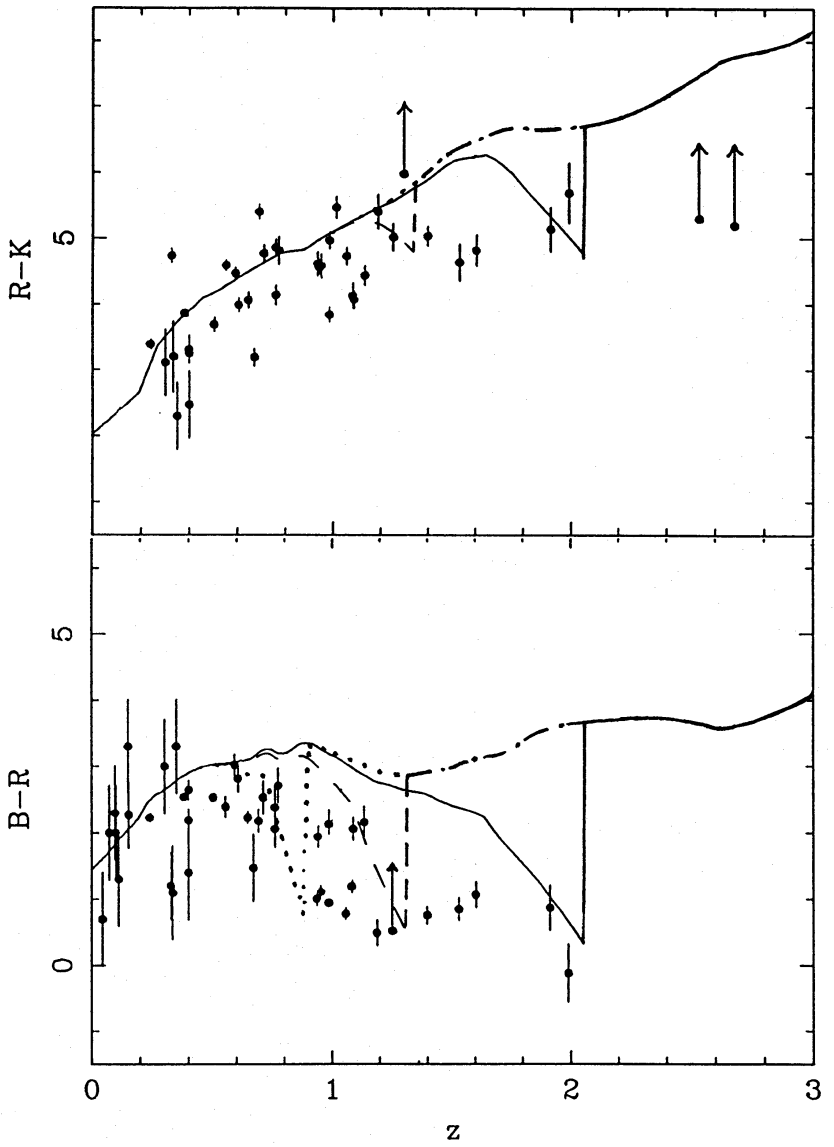

Figure 11. The effect on the $R-K$ and $B-R$ colour evolution of varying the epoch at which a small starburst (~ 0.01 the mass of the galaxy) occurs in an old ($z_f = 20$) passively evolving elliptical galaxy. The starbursts shown occur 5 Gyr (solid Line), 7 Gyr (dashed line) and 9 Gyr (dotted line) after the initial formation-epoch (corresponding to redshifts of $z \sim 2, 1.3, 0.9$). $\Omega_0 = 0$ and $H_0 = 50$ km s^{-1} Mpc^{-1} are assumed.

small bursts – a situation in effect indistinguishable from a μ model. A third alternative is a range of z_fs as considered above. Whatever the exact details, it is clear that the blue $R-K$ colours at low z can only be explained if a larger mass of the galaxy is involved in recent ($z \sim 2$) star-formation activity.

So, in summary, to model the scatter in $R-K$ the 'mean epoch' of bulk star formation must be varied by some means, either a range of z_fs or a range of star-formation histories. Having achieved this, any further blueing observed in $B-R$ can be reproduced by the further addition of 'small' starbursts.

4.4 CONSISTENCY OF THE MODELS WITH THE ESTIMATED REDSHIFTS

Finally, it remains to check whether the K-magnitude estimated redshifts used throughout this paper are consistent with the $K-z$ relations predicted by the models which have been found to

fit the colour evolution. The estimated redshifts were derived from the K–z relation described by Dunlop *et al.* (1989), which is defined empirically for galaxies brighter than $K \sim 17.5$. This relation is shown in Fig. 12 along with the 3C, 1-Jy and Selected Regions galaxy data on which it is based. Also shown are two alternative theoretical extrapolations of this relation in the region where it is poorly constrained by the data (i.e. $K > 17.5$). The dotted curve is the K–z relation predicted by the UV-Cold model with $z_f = 20$ ($\Omega_0 = 0$, $H_0 = 50$ km s^{-1} Mpc^{-1}), a model which provides a reasonable description of the loci followed by the data in both B–R/z and R–K/z diagrams (see Section 4.2). The resulting form of the K–z relation at high z is very similar to that used in deriving the estimated redshifts, thus indicating that the modelling of the colour/redshift data is internally consistent. The alternative, dashed curve in Fig. 12 is the K–z relation predicted by the UV-Cold model if it is formed at $z_f = 3.5$. The important point is that this younger model predicts that a galaxy with $K \sim 18$ should be practically at its formation redshift of 3.5. If the galaxy redshift estimates were altered to these high values, it would in fact be impossible to reconcile the model K–z relation with the resulting colour/redshift data. Use of the higher-z estimates would result in the galaxies on the R–K diagram with $z > 1.5$ all moving out to significantly higher redshifts. Since these galaxies are all fairly red ($R-K \sim 5$), this would simply strengthen the case for an old model being necessary to fit the optical–infrared colours. Only with relatively low redshift-estimates for the faintest objects is it possible to find a model which is consistent with both the K–z and colour/redshift diagrams. It may seem that the two Selected Regions galaxies with $z > 1$ have K magnitudes which contradict this statement: both are bright for their redshift, and in fact lie close to the $z_f = 3.5$ line on Fig. 12. This is, however, only to be expected when the spectroscopic data are so incomplete at high redshift, since the brightest objects tend to have their redshifts measured first. It is interesting that the one radio galaxy on the K–z diagram which has $z > 3$ (0903+34, $z = 3.395$, Lilly 1988), has a K magnitude consistent with the older models of spectral evolution.

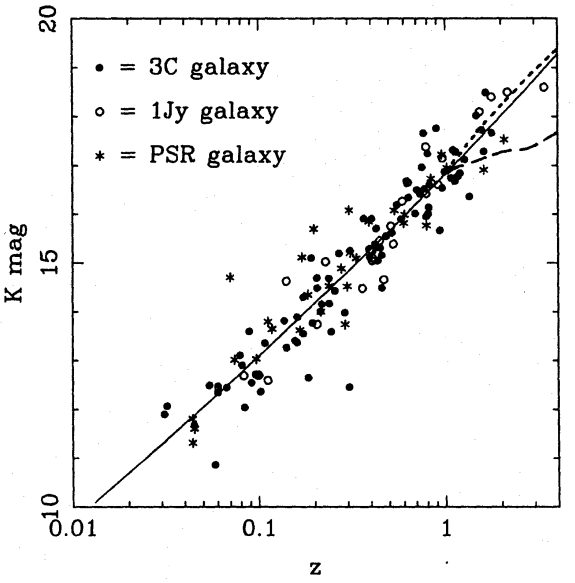

Figure 12. Alternative high-redshift extrapolations of the K–z relation for radio galaxies. The empirical K–z relation used for redshift estimation is shown (solid line) along with the data on which it is based –3CR galaxies (filled circles; Lilly & Longair 1984), 1-Jy galaxies (open circles; Lilly *et al.* 1985) and Selected Regions galaxies (asterisks; Dunlop *et al.* 1989). At high redshift, two alternative theoretical extrapolations of the K–z relation are also shown. These are derived from the UV-Cold model of galaxy evolution. The dotted line results from a formation redshift of $z_f = 20$, the dashed from $z_f = 3.5$ ($\Omega_0 = 0$, $H_0 = 50$ km s^{-1} Mpc^{-1}). The high-redshift form of the $z_f = 20$ K–z relation is clearly very similar to that used to derive the galaxy redshift estimates used in this study.

5 Conclusions

The main conclusions from the work described in this paper may be summarized as follows:

(i) *All* the radio galaxies in the sample show excess activity in $B-R$ relative to that expected from old (i.e $z_f \gtrsim 5$), passively evolving, 'Burst' models of galaxy evolution.

(ii) The reddest $R-K$ colours found in the sample can, however, only be reproduced by the models if the bulk of the stars in the galaxy formed ~ 18.5 Gyr ago. Such large ages cannot be accommodated in a closed Universe unless $H_0 < 35$ km s^{-1} Mpc^{-1}. Even in an empty Universe with $H_0 = 50$ km s^{-1} Mpc^{-1}, this implies a formation redshift as large as $z_f = 20$.

(iii) This conflict beween the optical and optical–IR colours means that it is extremely difficult to provide an adequate description of the data using models in which the star-formation rate is parameterized as a simple function of time [an old (18.5 Gyr) $\mu = 0.6$ model is just capable of fitting the red envelope in both $R-K$ and $B-R$, but this is clearly a struggle]. A better solution is to decouple the old and the new stellar populations and consider a two-component model. A successful fit to the red envelope in both $R-K$ and $B-R$ diagrams was achieved simply by adding a small, constant amount of UV flux (typical of that observed in present-day elliptical galaxies) to the old Burst model at all epochs. This result is interesting even if one rejects the idea that the UV flux is produced by young stars. In a sense, this Burst + UV model is actually the simplest, physically sensible model of minimum evolution – in a real galaxy there will always be some gas available for residual star-formation, unless the initial burst is perfectly efficient and the subsequent ejecta are blown out of the galaxy.

(iv) The blueward scatter in $B-R$ is relatively easy to model, with starbursts as small as 1 per cent of the galaxy mass being sufficient to account for the bluest optical colours in the sample, but the dispersion in $R-K$ cannot be explained by such relatively small differences in the star-formation histories of the galaxies. For a low-density Universe, the bluest $R-K$ colours found at $z \sim 1$ imply bulk star formation at $z \sim 2$, while (as stated above) the reddest colours can only be reproduced if the bulk of stars formed at $z > 10$ (assuming low Ω_0, the median redshift for bulk star formation is $z \simeq 5$, and ~ 10 per cent of objects require bulk star-formation at $z < 3$). Such variation in the mean epoch of bulk star-formation can be achieved either by assuming a range of formation redshifts $z_f \simeq 2$–20, or by assuming a common z_f but different star-formation histories. Any further blueing observed in $B-R$ can then be easily reproduced by the further addition of small ($\sim 10^9\ M_\odot$ Gyr^{-1}) short-lived (< 1 Gyr) starbursts occurring within ~ 1 Gyr of the time of observation.

Some of these conclusions have also been reached by other workers analysing different data with different models. A similar conflict between the ages implied by optical and optical–infrared colours was encountered by Spinrad & Djorgovski (1987) in attempting to describe the 3CR data using Bruzual's μ-models, while the age problem described in (ii) above has been encountered in several other studies (e.g. Hamilton, 1985; Windhorst *et al.* 1986), although not in such a severe form. This latter problem is, of course, intimately connected with the large globular cluster ages at present predicted by stellar evolution theory, since the galaxy models are based on theoretical tracks of stellar evolution. Thus, despite the attempt of the new models to include a more sophisticated treament of the GB and post-GB stages, it may be that problems still remain in the modelling of these phases. The models considered here assume uniform solar metallicity. This is justified on the basis that the metallicity is expected to approach this value and that, although the integrated photometry of a whole galaxy includes components of various metallicities (nucleus, spheroid, halo, disc), the average metallicity could be $\simeq$ solar. Nevertheless, it is clearly important to investigate the impact of variation in metallicity. This is being tested by combining the models of spectrophotometric evolution with a model of chemical evolution (Rocca-Volmerange & Schaeffer 1989).

It is interesting to compare our conclusions with the results of recent studies which have concentrated on obtaining more detailed information on smaller numbers of radio galaxies. The recent discovery by Lilly (1988) that the host galaxy of 0902+34 lies at $z=3.395$ and already possesses a clear 4000-Å break provides direct evidence that, in at least some radio galaxies, the bulk of the stars must form at $z>5$. Also, attempts to model the spectral energy distribution of this object have provided further support for the sort of two-component model which proved the most successful approach in the present study (Lilly 1988); if the UV-Cold model is adopted for 0902+34, extreme formation-redshifts ($z_f \geqslant 15$) and low Ω are required (Rocca-Volmerange & Guiderdoni 1989). In the case of this object, the large age estimates are based on the extent of the 4000-Å break and cannot, therefore, be attributed to any errors in the modelling of the Giant Branch.

Given the lower radio luminosity of the galaxies in the Selected Regions, the similarity of their spectral evolution to that of the 3CR galaxies could be regarded as an encouraging step in the direction of establishing that radio galaxies are representative probes of galaxy evolution. Indeed, Eisenhardt & Lebofsky (1987) (see also Lebofsky & Eisenhardt 1986) attempted to compare the colour evolution of radio-quiet and radio-loud ellipticals, and found no significant differences. However, their sample of radio-quiet ellipticals contained only two galaxies with $z>0.7$, whereas recent work has demonstrated that the UV component in some radio galaxies at higher redshift *does* seem to be related to the radio activity. McCarthy *et al.* (1987) and Chambers *et al.* (1987) have shown that, at least in the most powerful radio galaxies, the spatial distribution of the UV component often corresponds closely to that of the radio source. Furthermore, the recent discovery of a correlation between the level of UV light and radio spectral index (Lilly 1989) also supports the view that the radio activity and the optical properties of these galaxies are intimately related. Two possibilities for such a relation have been advanced: either in terms of jet-induced starbursts (as considered here) or in terms of scattered light from a hidden blazar (Tadhunter *et al.* 1989). The former explanation seems more plausible given the spectral shape of the observed near-UV light, which, even in the bluest cases, seems to approximate the form expected from a starburst. We cannot, at present, rule out a significant contribution by blazar light, but, unless this dominates the $R-K$ colours, the only impact on the conclusions presented here will be to assist in accounting for some of the bluest $B-R$ colours. It seems implausible that the R light could be dominated in this way, as the $B-R$ colours are nowhere near as blue as the $f_\nu \propto \nu^3$ spectrum to be expected on the scattered-light hypothesis. Young stars therefore appear the more probable explanation, but this still means that the importance of any link between star-formation activity and radio-source activity must be understood before the evolution of radio galaxies can be related to that of galaxies in general. Here we simply note that, given the relatively short lifetime of radio sources and the observed deficit of radio-source activity at $z \gtrsim 2$ (Dunlop & Peacock, in preparation), it seems highly unlikely that the bulk of the stars in these galaxies are produced as a result of radio-source activity.

At present, therefore, the evidence favours a picture in which the bulk of stars in radio galaxies are relatively old (i.e. formed at $z \gtrsim 5$), but there remains some residual star-formation which may be amplified by the most powerful radio sources. Given the multi-component structures of objects such as 3C368 observed by Djorgovski *et al.* (1987), the possibility remains that many radio galaxies at $z \sim 1.5$ are still *dynamically* young. If this proved to be the case, it would strongly support hierarchical models of galaxy formation in which pre-galactic stars form in systems of $\ll 10^{11}\ M_\odot$ (e.g. the 'standard' Cold Dark Matter model). It is unfortunate that the more recent star-forming activity has tended to confuse the observational situation; detailed infrared imaging of high-redshift radio galaxies should be the best way of settling this fundamental question.

Acknowledgments

JSD acknowledges financial support from the Royal Society of Edinburgh via the Robert Cormack Bequest studentship.

References

Borsenberger, J. & Gros, M., 1978. *Astr. Astrophys. Suppl.*, **31,** 291.
Bruzual, G., 1983a. *Astrophys. J.*, **273,** 105.
Bruzual, G., 1983b. *Rev. Mex. Astr. Astrofis.*, **8,** 63.
Bruzual, G., 1985. *Rev. Mex. Astr. Astrofis.*, **10,** 55.
Bruzual, G. & Kron, R. G., 1980. *Astrophys. J.*, **241,** 25.
Chambers, K. C., Miley, G. K. & Joyce, R. R., 1988. *Astrophys. J.*, **329,** L79.
Chambers, K. C., Miley, G. K. & van Breugel, W., 1987. *Nature*, **329,** 604.
Chokshi, A. & Wright, E. L., 1987. *Astrophys. J.*, **319,** 44.
Djorgovski, S., Spinrad, H. Pedelty, J., Rudnick, L. & Stockton, A. 1987. *Astr. J.*, **93,** 1307.
Downes, A. J. B., Peacock, J. A. Savage, A. & Carrie, D. R., 1986. *Mon. Not. R. astr. Soc.*, **218,** 31.
Dunlop, J. S., Peacock, J. A., Savage, A., Lilly, S. J., Heasley, J. N. & Simon, A. J. B., 1989. *Mon. Not. R. astr. Soc.*, **238,** 1171.
Eisenhardt, P. R. M. & Lebofsky, M. J., 1987. *Astrophys. J.*, **316,** 70.
Engels, D., Sherwood, W. A., Wamsteker, W. & Schultz, G. V., 1981. *Astr. Astrophys. Suppl.*, **45,** 5.
Frogel, J. A., Persson, S. E., Aaronson, M. & Matthews, K., 1978. *Astrophys. J.*, **220,** 75.
Gratton, R. G., 1985. *Astr. Astrophys.*, **147,** 169.
Guiderdoni, B. & Rocca-Volmerange, B., 1987. *Astr. Astrophys.*, **186,** 1.
Guiderdoni, B. & Rocca-Volmerange, B., 1988. *Astr. Astrophys. Suppl.*, **74,** 185.
Gunn, J. E. & Oke, J. B., 1975. *Astrophys. J.*, **195,** 255.
Gunn, J. E. & Stryker, L. L., 1983. *Astrophys. J. Suppl.*, **52,** 121.
Hamilton, D., 1985. *Astrophys. J.*, **297,** 371.
Hayes, D. S. & Latham, D. W., 1975. *Astrophys. J.*, **197,** 593.
Huchra, J. P., 1977. *Astrophys. J.*, **217,** 928.
Johnson, H. L., 1966. *Ann. Rev. Astr. Astrophys.*, **4,** 193.
Kjaergaard, P., 1987. *Astr. Astrophys.*, **178,** 210.
Lebofsky, M. J. & Eisenhardt, P. R. M., 1986. *Astrophys. J.*, **300,** 151.
Lee, T. A., 1970. *Astrophys. J.*, **162,** 217.
Lilly, S. J., 1988. *Astrophys. J.*, **333,** 161.
Lilly, S. J., 1989. *Astrophys. J.*, **340,** 77.
Lilly, S. J. & Longair, M. S., 1984. *Mon. Not. R. astr. Soc.*, **211,** 833.
Lilly, S. J., Longair, M. S. & Allington-Smith, J. R., 1985. *Mon. Not. R. astr. Soc.*, **215,** 37.
Lilly, S. J. McLean, I. S. & Longair, M. S. 1984. *Mon. Not. R. astr. Soc.*, **209,** 401.
McCarthy, P. J., van Breugel, W., Spinrad, H. & Djorgovski, S., 1987. *Astrophys. J.*, **321,** L29.
Maeder, A., 1981. *Astr. Astrophys.*, **102,** 401.
Mihalas, D., 1972. *NCAR Technical Note*, **STR76.**
Miller, G. E. & Scalo, J. M., 1979. *Astrophys. J. Suppl.*, **41,** 513.
Mountain, C. M., Leggett, S. K., Selby, M. J., Blackwell, D. E. & Petford, A. D., 1985. *Astr. Astrophys.*, **151,** 399.
Ratcliff, S. J., 1987. *Astrophys. J.*, **318,** 196.
Renzini, A., 1981. *Ann. Phys. Fr.*, **6,** 87.
Renzini, A. & Buzzoni, A., 1986. in: *Spectral Evolution of Galaxies*, p. 195, eds Chiosi, C. & Renzini, A., Reidel, Dordrecht.
Rocca-Volmerange, B., 1989. *Mon. Not. R. astr. Soc.*, **236,** 47.
Rocca-Volmerange, B. & Guiderdoni, B., 1987. *Astr. Astrophys.*, **175,** 15.
Rocca-Volmerange, B. & Guiderdoni, B., 1988. *Astr. Astrophys. Suppl.*, **75,** 93.
Rocca-Volmerange, B. & Guiderdoni, B., 1989. In: *The Epoch of Galaxy Formation,* p. 387, eds Frenk, C. S., Ellis, R. S., Shanks, T., Heavens, A. F. & Peacock, J. A. Kluwer, Dordrecht.
Rocca-Volmerange, B. & Schaeffer, R., 1989. *Astr. Astrophys.*, submitted.
Salpeter, E. E., 1955. *Astrophys. J.*, **121,** 161.
Scalo, J. M., 1986. *Fundam. Cosmic Phys.*, **11,** 1.
Schneider, D. P., Gunn, J. E. & Hoessel, J. G., 1983. *Astrophys. J.*, **268,** 476.
Searle, L., Sargent, W. L. W. & Bagnuolo, W., 1973. *Astrophys. J.*, **179,** 427.

Spinrad, H., 1986. *Publs astr. Soc. Pacif.*, **98,** 269.
Spinrad, H. & Djorgovski, S., 1987. *Observational Cosmology, IAU Symp. No. 124,* p. 129, eds Hewitt, A., Burbidge, G. & Fang, L. Z., Reidel, Dordrecht.
Sweigart, A. V. & Gross, P. G., 1978. *Astrophys. J. Suppl.*, **36,** 405.
Tadhunter, C. N., Fosbury, R. A. E. & di Serego Alighieri, S., 1989. in: *Como workshop on BL Lac Objects: 10 Years After*, in press.
Tinsley, B. M., 1967. *PhD thesis*, University of Texas.
Tinsley, B. M., 1972. *Astr. Astrophys.*, **20,** 383.
Tinsley, B. M., 1980. *Astrophys. J.*, **241,** 41.
Tinsley, B. M. & Gunn, J. E., 1976. *Astrophys. J.*, **203,** 52.
Windhorst, R. A., Koo, D. C. & Spinrad, H., 1986. in: *Galaxy Distances and Deviation from Universal Expansion, NATO Advanced Research Workshop*, p. 197, eds Madore, B. F. & Tully, R. B., Reidel, Dordrecht.
Windhorst, R. A., Dressler, A. & Koo, D. C., 1987. *Observational Cosmology, IAU Symp. No. 124,* p. 573, eds Hewitt, A., Burbidge, G. & Fang, L. Z., Reidel, Dordrecht.
Wu, C. C., Faber, S. M., Gallagher, J. S., Peck, M. & Tinsley, B. M., 1980. *Astrophys. J.*, **237,** 290.